(This is a sample cover image for this issue. The actual cover is not yet available at this time.)

Quaternary Science Reviews 64 (2013) 76–89

Contents lists available at SciVerse ScienceDirect

Quaternary Science Reviews

journal homepage: www.elsevier.com/locate/quascirev

Modern and Holocene aeolian dust variability from Talos Dome (Northern Victoria Land) to the interior of the Antarctic ice sheet

B. Delmonte [a,*], C. Baroni [b,c], P.S. Andersson [d], B. Narcisi [e], M.C. Salvatore [b], J.R. Petit [f], C. Scarchilli [e], M. Frezzotti [e], S. Albani [a], V. Maggi [a]

[a] DISAT – Department of Earth and Environmental Sciences, University Milano-Bicocca, Piazza della Scienza 1, 20126 Milano, Italy
[b] Dipartimento di Scienze della Terra, Università di Pisa, Via S. Maria 53, 56126 Pisa, Italy
[c] CNR, Istituto di Geoscienze e Georisorse, Via S. Maria 53, 56126 Pisa, Italy
[d] LIG – Laboratory for Isotope Geology, Swedish Museum for Natural History, Box 50007, 104 05 Stockholm, Sweden
[e] ENEA, CR Casaccia, SP. Anguillarese, 301, I-00123 Roma, Italy
[f] LGGE-CNRS-Université Joseph Fourier, UMR 51230, BP 96, 38402 St Martin d'Hères Cedex, France

ARTICLE INFO

Article history:
Received 28 June 2012
Received in revised form
19 November 2012
Accepted 30 November 2012
Available online

Keywords:
Dust
Antarctica
Holocene
Ice cores
Sr–Nd isotopes

ABSTRACT

High-elevation sites from the inner part of the East Antarctic plateau sample windborne dust representative of large portions of the Southern hemisphere, and are sensitive to long-range atmospheric transport conditions to polar areas. On the periphery of the ice sheet, conversely, the aeolian transport of particles from high-elevation ice-free areas can locally represent a relatively important additional input of dust to the atmosphere, and the interplay of atmospheric dynamics, dust transport and deposition is strictly related to the regional atmospheric circulation behaviour both at present-day and in the past. The understanding of the spatial extent where local sources can influence the mineral dust budget on the ice sheet is fundamental for understanding the atmospheric dust cycle in Antarctica and for the interpretation of the dust history in marginal glaciological settings.

In this work we investigate the spatial variability of dust flux and provenance during modern (pre-industrial) and Holocene times along a transect connecting Talos Dome to the internal sites of the Antarctic plateau and we extend the existing documentation of the isotopic (Sr–Nd) fingerprint of dust-sized sediments from Victoria Land source areas.

Dust flux, grain size and isotopic composition show a marked variability between Talos Dome, Mid Point, D4 and Dome C/Vostok, suggesting that local sources play an important role on the periphery of the ice sheet. Microscope observations reveal that background mineral aerosol in the TALDICE core is composed by a mixture of dust, volcanic particles and micrometric-sized fragments of diatoms, these latter representing a small but pervasive component of Antarctic sediments. A set of samples from Victoria Land, mostly consisting of regolith and glacial deposits from high-elevation areas, was collected specially for this work and the isotopic composition of the dust-sized fraction of samples was analyzed. Results reveal a close relationship with the parent lithologies, but direct comparison between source samples and firn/ice core dust is problematical because of the ubiquitous volcanic contribution to the environmental particulate input in the Talos Dome area.

The frequency of events potentially suitable for peripheral dust transport to Talos Dome appears relatively high for present-day conditions, according to back trajectories calculations, and the related air flow pattern well-defined from a seasonal and spatial perspective. Also, as expected from palaeo-data, these events appear extremely uncommon for internal sites.

1. Introduction

The aeolian deflation of continents and the mineral dust transport long-range responded to the major climate and environmental changes during the Quaternary (e.g. Petit et al., 1999; Lambert et al., 2008; Maher et al., 2010). Dust particles can be transported around the globe in suspension in the troposphere at a wide variety of heights, and their deposits can be far away from their origins (Kohfeld and Harrison, 2001). The long and detailed aeolian sequences obtained from ice cores drilled onto the interior of the Antarctic ice sheet allowed assessing the past atmospheric

* Corresponding author. Tel.: +39 02 6448 2847; fax: +39 02 6448 2895.
E-mail address: barbara.delmonte@unimib.it (B. Delmonte).

0277-3791/$ – see front matter © 2012 Elsevier Ltd. All rights reserved.
http://dx.doi.org/10.1016/j.quascirev.2012.11.033

circulation variability on a variety of timescales and the related environmental changes that occurred at high southern latitudes (Petit et al., 1999; Lambert et al., 2008). During glacial/interglacial cycles, most of the variability in dust concentration in central East Antarctica (Vostok, Dome C) was related to the supply of small mineral particles from the remote continental sources, to the snow accumulation rate, and to the atmospheric transport efficiency (lifetime of aerosol), all factors related to temperature and to the hydrological cycle (Petit and Delmonte, 2009).

On the periphery of the Antarctic plateau, an additional input of fine dust particles to the atmosphere and to the ice sheet can derive from ice-free terrains frequently occurring in mountain ranges or protruding above the ice sheet surface as nunataks (e.g. Tedrow and Ugolini, 1966). The supply of sediments from proximal sources was likely faint or nil for inner, high elevation sites such as Vostok and Dome C both during glacial periods, when the dust signature is consistent with a South American origin (Grousset et al., 1992; Basile et al., 1997; Delmonte et al., 2008; Gabrielli et al., 2010; Vallelonga et al., 2010), and during the Holocene, when dust is believed to derive from multiple remote sources (Revel-Rolland et al., 2006; Marino et al., 2009; Gabrielli et al., 2010). Conversely, the contribution from these areas may become important for peripheral areas (Bory et al., 2010; Delmonte et al., 2010a; Albani et al., 2012a), in particular those that are close to the Transantarctic Mountains, that represent the sole extensive area with important rock outcrops in this sector of East Antarctica. Under cold climate conditions such as those of Antarctica, moreover, it is known that dust mass transport rates may be significantly higher than for the equivalent wind speed in warm and hot climates, in relation to the extremely low air humidity, to air density and turbulence (McKenna Neuman, 2004); thus, the export of sediments from Antarctic ice-free terrains can be relevant. Furthermore, even small amounts of dust have the potential to influence the overall budget in low deposition environments such as the East Antarctic ice Sheet.

At the site of Talos Dome, located in the Ross Sea sector of East Antarctica in Northern Victoria Land (Frezzotti et al., 2007), some physical-chemical properties of dust (grain size, concentration, Sr–Nd isotopic composition) suggested a contribution from local sources, mostly represented by unconsolidated Pleistocene glacial deposits and regolith located at high elevation and outcropping above the ice sheet surface in Victoria Land (Delmonte et al., 2010a). Data also suggested that this local contribution was relatively more important during the Holocene – at a time when the remote dust input was extremely low – with respect to the Last Glacial period (Albani et al., 2012a).

Under the peculiar conditions of the Talos Dome site, the entrainment and transport of local dust particles to the site is influenced by local meteorological conditions, in turn related to regional climate (Albani et al., 2012a). Thus, the dust and climate record from the uppermost 670 m of the ~1620 m deep TALDICE (TALos Dome Ice CorE drilling project) ice core (Stenni et al., 2011) offers an extraordinary opportunity to investigate in detail the regional atmospheric circulation changes during the Holocene and their relationship with the deglaciation history of the Ross Sea.

Despite the demonstrated importance of aeolian dust transport to Antarctica, still little information exists on the entrainment, transport and deposition of mineral aerosol from marginal ice-free areas towards the Antarctic interior, one major difficulty consisting in the extremely low dust concentration in firn and ice cores during interglacial climate conditions (Petit and Delmonte, 2009). In order to form a better view of the spatial extent where peripheral, high-elevation dust sources can play a significant role with respect to the mineral dust input on the ice sheet during modern (pre-industrial) times, we investigate in this work the flux, grain size and $^{87}Sr/^{86}Sr$–$^{143}Nd/^{144}Nd$ isotopic composition of aeolian dust from different firn and ice cores drilled along a transect from Talos Dome all through the interior of the ice sheet (Dome C – Vostok area, Fig. 1a). These measurements are complemented by a number of microscopic (SEM) morphological observations that provide fundamental indications for data interpretation. In addition, the isotopic composition of the dust-sized fraction of sediments collected for this study in some target potential source areas located inside northern Victoria Land (NVL) and southern Victoria Land (SVL) is presented. This work represents the expansion of a former study (Delmonte et al., 2010a), and a contribution to the documentation of local mineral aerosol fingerprint, which can be of use for the interpretation of dust origin in peripheral East Antarctica in the past. We also investigate the modern frequency and pathways of air masses flowing from Victoria Land potential source areas (PSAs) to the selected drilling sites in order to obtain a first assessment of the occurrence of events potentially suitable for peripheral dust transport and an overview of air mass flow paths at present-day, which can be compared with evidences from palaeo-data.

2. Materials and methods

This study was carried out in different steps:

1. Sampling of firn cores and dust measurements
2. Field sampling of PSAs in Antarctica, sample preparation

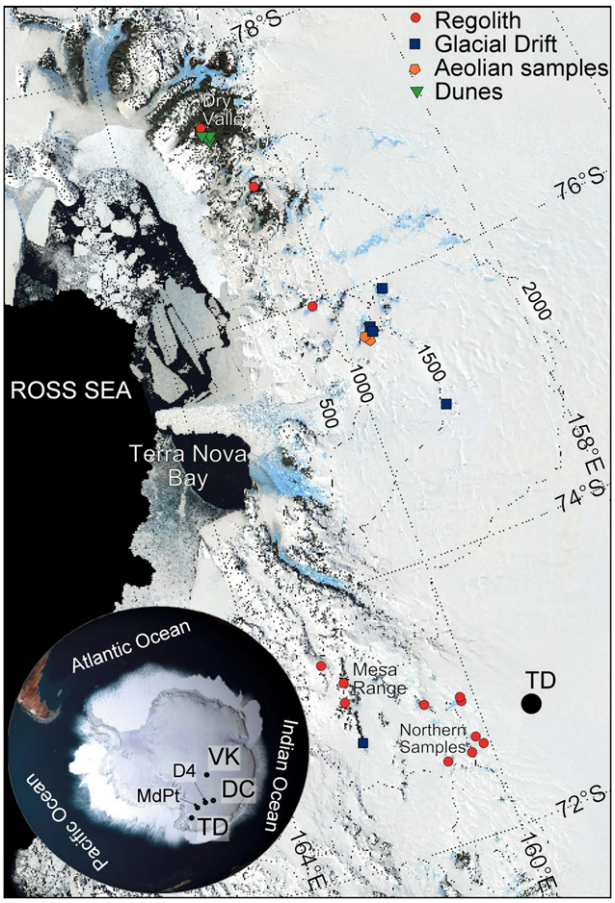

Fig. 1. Satellite image (Landsat image mosaic of Antarctica project) of Victoria land with indication of the TALDICE ice core drilling site at Talos Dome (TD), typology and location of the dust source samples analyzed for Sr and Nd isotopic composition (this work and Delmonte et al., 2010a) and topography. Insert: Antarctica and ice core drilling sites mentioned in the text. TD (Talos Dome), MdPt (Mid Point), D4, DC (Dome C), VK (Vostok).

3. Microscope observations
4. Isotopic analyses
5. Air mass back-trajectories calculations

2.1. Firn sampling

Four firn cores aligned along an array from Talos Dome to Dome C, passing through Mid Point and D4 (Fig. 1a) were selected for this study. The transect, spanning more than 1400 km, starts at an elevation of 2315 m a.s.l. and reaches a maximum elevation of 3230 m at Dome C. A detailed study of the surface mass balance in the area together with a description of the morphological and climatological characteristics of the sites is provided by Frezzotti et al. (2004, 2005, 2007). These studies provide also the literature source for local accumulation and elevation data reported in Table 1.

According to core availability, firn samples were selected from below the depth of the Tambora (1816 A.D.) volcanic marker; the age interval of samples from each site is reported in Table 1. In this work we refer to "modern" or "pre-industrial" samples in relation to firn core samples spanning a time interval between the early 15th and the 19th centuries, which include the time period known as the *Little Ice age* during which glaciers advanced also in Victoria Land (Baroni and Orombelli, 1994; Hall, 2009).

2.1.1. Talos Dome

Talos Dome (TD, 72°48′S, 159°06′E, 2315 m a.s.l) is an ice dome located on the periphery of the East Antarctic ice sheet (Fig. 1), ca 290 km from the Southern Ocean and 250 km from the Ross Sea (Frezzotti et al., 2007). Between 2004 and 2007, a deep drilling carried out in the framework of the *TALos Dome Ice CorE drilling project* (**TALDICE**) led to the recovery of 1620 m of ice, spanning ~250 ka (Stenni et al., 2011). In this work we analyzed a set of 9 *bags* (i.e. 1-m long, 90-° "cut-A" sections) selected from the upper (firn) part of the core (30–70 m depth) spanning the period from 1420 A.D. to about 1810 A.D. (Buiron et al., 2011; Severi et al., 2012).

A dry decontamination procedure for firn was adopted at LGGE-CNRS Laboratory (Grenoble, France) in cold room under laminar flow bench. After scraping away the outer part of each core with a ceramic knife, about 9–10 sub-samples were obtained from each *bag*. These were inserted in clean Corning® centrifuge tubes and melted in clean room at ambient temperature. Dust concentration and grain size analysis was performed with a Multisizer IIe Coulter Counter set for measurements of particles with equivalent spherical diameters between 0.7 and 20 μm, following the procedure described in Delmonte et al. (2002).

Dust concentration data obtained from sub-samples of the same section were then averaged (see supplementary information) and the mean value was assigned to each bag.

2.1.2. ITASE cores: mid point, D4, Dome C

In the framework of the *International TransAntarctic Scientific Expedition* (ITASE) project and as part of the Franco-Italian activities at Concordia Station between 1998 and 2000, some shallow cores were drilled in the E-NE part of the Dome C drainage area and in Northern Victoria Land. Three cores recovered as part of that study were made accessible for this project:

- The Mid Point (MdPt) core (75°32′S, 145°51′E; 2454 m a.s.l.);
- The D4 core (75°35′S, 135°49′E, 2793 m a.s.l.);
- The Dome C (DC) core (75°06′S; 123°21′E; 3230 m a.s.l.).

Samples for this work were selected from below the depth of the Tambora eruption (1816 A.D.) identified in each core (Frezzotti et al., 2005) by means of characteristic non-sea-salt (nss) SO_4^{2-} spikes. The MdPt core was sampled from 16 to 28 m depth (17 sections; 1620–1800 A.D.); the D4 core from 18 to 30 m depth (22 sections, 1420–1700 A.D.); the DC core from 12.5 to 24.5 m depth (21 sections; 1570–1800 A.D.). Firn sections (with density between 450 and 600 kg m^3) consisted of entire cores, i.e. 360° transversal sections, with only a few exceptions where half-cores (180° transversal sections) were available. Decontamination was performed at DISAT (Milano-Bicocca University) following the same procedure adopted at LGGE, while dust concentration and size measurements were performed by using a Multisizer™ 3 Coulter Counter® analyzing particles from 1 to 30 μm. For each core, a ~15–20 ml aliquot was dedicated to particle analysis, while the residual liquid was preserved in pre-cleaned Savillex PFA jars, and subsequently filtered on a Nuclepore™ track-etched membrane (porosity 0.4 μm). Re-suspension of dust from the membranes was then achieved through sonication, as in Delmonte et al. (2010a).

2.2. Victoria Land PSA sampling and sample preparation

Glacial deposits and glacially shaped bedrock preserved in Antarctic ice-free areas offer valuable potential for identifying PSAs at the margin of the ice sheet. Sampling sites were selected taking into account the Cenozoic glacial history and the landscape assemblage of Victoria Land depicted by previous geological and geomorphological studies (e.g. Orombelli et al., 1990; Armienti and Baroni, 1999; Meneghel et al., 1999; Baroni et al., 2004, 2005, 2008 and references therein). New potential key sites were also selected through geomorphological survey in the Outback Nunatak area (Northern Victoria Land) during the 2009/2010 Antarctic field season. On the basis of results from a former study (Delmonte et al., 2010a), the sampling strategy was principally focused in finding high-elevation sites affected by old glacial deposits and relict surfaces with well-developed regolith (incoherent mantle of weathered, disintegrated rock fragments resting upon solid bedrock, possibly with old soils on top), which could represent source for

Table 1
Site and dust data.

Firn core	Elevation (m a.s.l.)	Acc. rate (cm w.eq./yr)	Firn sections	Time period	1–5 μm particles ppb (±st.dev)	1–5 μm particles (mg m^{-2} yr^{-1}) (±st.dev)	5–10 μm particles (ppb) (±st.dev)	5–10 μm particles (mg m^{-2} yr^{-1}) (±st.dev)
Talos Dome (TALDICE) 72°48′S, 159°06′E	2315	8.7 ± 0.8	90	1420–1810 A.D.	8 (±4)	0.75 (±0.35)	**4** (±3)	0.35 (±0.26)
Mid point (MdP-A) (ITASE) 75°32′S, 145°51′E	2455	3.6 ± 1.8	17	1620–1800 A.D.	14 (±3)	0.50 (±0.27)	**4** (±2)	0.14 (±0.10)
D4 (ITASE) 75°35′S, 135°49′E	2795	2.0 ± 1.1	22	1420–1700 A.D.	9 (±4)	0.19 (±0.13)	**3** (±2)	0.05 (±0.05)
DC (ITASE) 75°06′S, 123°21′E	3230	2.5 ± 1.3	21	1570–1800 A.D.	8 (±4)	0.20 (±0.14)	**1** (±1)	0.03 (±0.03)

Columns 1, 2, 3: Firn cores analyzed in this work with coordinates of drilling site, elevation, mean accumulation rate (Frezzotti et al., 2004, 2005; Buiron et al., 2011) for pre-industrial conditions. Columns 4 and 5: Number of firn core sections analyzed in this work and integrated time period spanned by the cores. Columns 6, 7: Concentration (±st.dev.) and flux (±st.dev.) of particles with diameter between 1 and 5 μm and between 5 and 10 μm.

Table 2
Isotopic composition of pre-industrial and Holocene firn and ice core dust samples from East Antarctica.

Dust sample	Climatic period	$^{87}Sr/^{86}Sr$	$\pm 2\sigma_{mean} * 10^{-6}$	$\pm 2\sigma * 10^{-6}$	$^{87}Sr/^{86}Sr$ normalized	$^{143}Nd/^{144}Nd$	$\pm 2\sigma_{mean} * 10^{-6}$	$\varepsilon_{Nd}(0)$	$\pm 2\sigma$	Reference
Dome C (firn)	1570–1800 A.D.	0.707440	20	20	0.707468	0.512438	64	−3.90	1.2	This work
D4 (firn)	1420–1700 A.D.	0.708440	13	16	0.708468	n.d.	n.d.	n.d.	n.d.	This work
Mid Point (firn)	1620–1800 A.D.	0.707526	47	47	0.707554	0.512482	89	−3.04	1.7	This work
EPICA-Dome C (ice)_1	Holocene	0.710013	55	n.d.		0.512407	101	−4.51	1.97	Delmonte et al. (2007)
EPICA-Dome C (ice)_2	Holocene	0.709435	37	n.d.		0.512347	95	−5.68	1.85	Delmonte et al. (2007)
Vostok (ice)_1	Holocene	0.711200	35	n.d.		0.512126	17	−9.99	0.3	Basile (1997), Delmonte et al. (2007)
Vostok (ice)_2	Holocene	0.709289	50	n.d.		0.512379	44	−5.05	0.9	Basile (1997), Delmonte et al. (2007)
Talos Dome (ice)_1	Holocene	0.708437	14	16		0.512510	180 (Ψ)	−2.5	3.5	Delmonte et al. (2010a)
Talos Dome (ice)_2	Holocene	0.707689	15	16		0.512643	32	+0.1	0.6	Delmonte et al. (2010a)

Columns 1, 2: Firn and ice core dust samples and age of the dust samples analyzed. Columns 3, 4, 5, 6: $^{87}Sr/^{86}Sr$ isotopic composition of samples, $\pm 2\sigma_{mean} * 10^{-6}$ (internal precision, 2 standard errors of the mean), $\pm 2\sigma * 10^{-6}$ (external precision). The external precision for $^{87}Sr/^{86}Sr$ as judged from running 200 ng loads of 987 standard is 16 ppm ($n = 33$), while loads in the range 10–50 ng result in a precision of 22 ppm ($n = 12$). Internal precision is used if it exceeds the external (Deines et al., 2003). Normalized $^{87}Sr/^{86}Sr$ ratios from this work were corrected corresponding to a value of 0.710245 for NBS 987 standard (NBS 987 litt.0.710245; LIG 0.710217; Difference 0.000028). Columns 7, 8: $^{143}Nd/^{144}Nd$ isotopic composition $\pm 2\sigma_{mean} * 10^{-6}$ (internal precision, 2 standard errors of the mean). Accuracy correction was not necessary since the mean $^{143}Nd/^{144}Nd$ ratio for nNdβ standard was 0.511895 ± 22 ($n = 20$). Columns 9, 10: Nd isotopic ratios expressed as epsilon units given with uncertainty estimates based upon external precision for standard runs. Internal precision is used if it exceeds the external (Deines et al., 2003). The external precision for $^{143}Nd/^{144}Nd$ as judged from values for 4–12 ng loads of nNdβ standard was 43 ppm. Corresponding values for >200 ng loads of La Jolla standard are 9.2 ppm and 0.5118484 ± 4.7 ($n = 32$). Accuracy correction was not necessary since the mean $^{143}Nd/^{144}Nd$ ratio was 0.511895 ± 22 ($n = 20$). $\varepsilon_{Nd}(0) = [(^{143}Nd/^{144}Nd)_{sample}/(^{143}Nd/^{144}Nd)_{CHUR} - 1] \cdot 10^4$; CHUR: CHondritic Uniform Reservoir, with $^{143}Nd/^{144}Nd = 0.512638$. Column 11: reference for data. (Ψ) Enlarged error due to technical problem. n.d. = no data.

loose sediments available for wind transport and still undocumented from a geochemical point of view.

Therefore, we selected sites carrying relict landscape features that document a continuous and long lasting exposure to weathering as documented by surface exposure dating conducted in key sites (Schafer et al., 1999; Summerfield et al., 1999; Oberholzer et al., 2003, 2008; Di Nicola et al., 2009; Strasky et al., 2009).

Additional fieldwork was carried out in the McMurdo Dry Valleys, given the well-recognized importance of those areas in mineral dust generation (e.g. Lancaster, 2002).

According to their geographic provenance, four different groups -or families of PSA samples (Table 3) were collected. These are (1) the northern samples (**NTH** in Table 3), collected on the Outback Nunataks in Northern Victoria Land, located E-NE from Talos Dome (Fig. 1), (2) the McMurdo Dry Valleys (**DRV** in Table 3), (3) the intermediate hills (**IH** in Table 3) between the Outback Nunataks and the Mesa Range (only one sample from this group was analyzed in this work), and (4) extremely inaccessible remote nunataks on the polar plateau (**PNTK** in Table 3).

Among the six samples belonging to the NTH family, two were collected on the Frontier Mountains, a nunatak rising about 600 m above the regional ice sheet level. One of these, NTH_1, consists of regolith developed 3179 m a.s.l. on granite, NTH_2 consists of a granitic glacial drift collected 2606 m a.s.l. Other samples from this group include regolith NTH_3 developed on granite and collected 2920 m a.s.l. on the Miller Butte, regolith NTH_4 developed on Ferrar dolerite and collected 3059 m a.s.l. on the Roberts Butte, regolith NTH_5 from metamorphosed beacon sandstone collected 2740 m a.s.l. on Mt. Bower, and regolith NTH_6 developed on Priestley Schist (Wilson Terrane) and collected about 2580 m a.s.l. on Mt. Weihoupt.

Among samples from the DRV family, DRV_5 and DRV_6, both developed on Ferrar dolerite, were collected 1780 and 1332 m a.s.l., respectively on Mt. Gran and on Mt. Peleus, in the Olympus Range. In addition, a set of sand samples from barchan and whaleback dunes from the Victoria Valley (350–420 m a.s.l., Bristow et al., 2010a,b, 2011) was made available for this study (*courtesy of P. Augustinus*). The optically stimulated luminescence (OSL) ages of these dune deposits indicate they are modern to 320 ± 80 years old. Each sample was free from organic matter and carbonates, which was formerly removed with hydrogen peroxide and HCl, respectively (*P. Augustinus, pers. comm.*). In the specific case of Victoria Valley, sand dunes are believed to be mostly inherited from sandstone units of the Beacon Supergroup (e.g Calkin and Rutford, 1974).

Among samples from the IH group we selected only one sample collected from the top of Sequence Hills about 2635 m a.s.l., consisting of regolith developed on Ferrar dolerite, at a site characterized by evident tors and abundant sandy sediments. Finally, sample PNTK_1 collected 1720 m a.s.l. on the extremely inaccessible Mount Kring was selected for this study. Mt. Kring is an isolated nunatak emerging more than 200 m on the East Antarctic plateau located within the upper David Glacier basin in Oates Land (SVL) at about 150 km from the coast. The sample represents the matrix of a Late Pleistocene glacial drift; parent lithologies are Beacon sandstone, Ferrar dolerite and Kirkpatrick basalts.

All sediment samples were handled in a dedicated environment (class 10,000 clean room) available at DISAT (Milano Bicocca University). Particles with equivalent spherical diameter smaller than 5 μm were selected through humid sedimentation as in former studies (Delmonte et al., 2010a), checking dust size by Coulter Counter® Multisizer™ 3. After size separation, dust was filtered on a Nuclepore™ track-etched membrane in order to remove soluble compounds, and was then re-suspended through sonication.

2.3. Microscope observations

Scanning Electron Microscope (SEM) qualitative morphological observations were carried out on a set of 20 Holocene samples from the Talos Dome TALDICE ice core deriving from 25-cm long *dust strips* representing about 3 years of accumulation in the ice core. All samples were formerly analyzed for particle concentration and grain size (Albani et al., 2012a). Aliquots were selected in order to

Table 3
Sr and Nd isotopic composition of Victoria land source samples analyzed in this work.

Sample name	Geographic coordinates	Elevation (m a.s.l.)	Area	Material (substrate)	$^{87}Sr/^{86}Sr$	$\pm2\sigma_{mean} * 10^{-6}$	$\pm2\sigma * 10^{-6}$	$^{87}Sr/^{86}Sr$ normalized*	$^{143}Nd/^{144}Nd$	$\pm2\sigma_{mean} * 10^{-6}$	$\varepsilon_{Nd}(0)$	$\pm2\sigma$
NTH_1	72°59′16″S, 160°20′50″E	3179	Frontier Mountains	Regolith (granite)	0.725328	06	11	0.725356	0.512405	05	−4.5	0.10
NTH_2	72°58′29″S, 160°21′29″E	2606	Frontier Mountains	Glacial drift (granite)	0.745529	09	11	0.745557	0.512387	07	−4.9	0.13
NTH_3	72°42′09″S, 160°14′15″E	2920	Miller Butte	Regolith (granite)	0.798656	22	22	0.798684	0.512216	07	−8.2	0.3
NTH_4	72°39′04″S, 160°07′20″E	3059	Roberts Butte	Regolith (Ferrar dolerite)	0.712184	17	17	0.712212	0.512386	05	−4.9	0.3
NTH_5	72°36′45″S, 160°30′29″E	2740	Mt. Bower	Regolith (beacon sandstone, metamorphosed)	0.718124	08	11	0.718152	0.512348	04	−5.6	0.10
NTH_6	72°36′01″S, 161°03′27″E	2580	Mt. Weihoupt	Regolith (shist)	0.721112	07	11	0.721140	0.512004	08	−12.4	0.2
DRV_1	77°22′19″S, 162°10′39″E	400	Dry Valleys	Dune (beacon sandstone)	0.712120	07	11	0.712148	0.512222	19	−8.1	0.4
DRV_2	77°22′21″S, 162°10′57″E	400	Dry Valleys	Dune (beacon sandstone)	0.712216	08	11	0.712244	0.512249	16	−7.6	0.4
DRV_3	77°22′22″S, 161°55′18″E	420	Dry Valleys	Dune (beacon sandstone)	0.712677	09	11	0.712705	0.512244	10	−7.7	0.3
DRV_4	77°22′44″S, 162°9′52″E	350	Dry Valleys	Dune (beacon sandstone)	0.712930	05	11	0.712705	0.512246	06	−7.6	0.2
DRV_5	76°55′58″S, 161°02′50″E	1780	Dry Valleys (Mt. Gran)	Regolith (Ferrar dolerite)	0.713708	05	11	0.713736	0.512344	06	−5.7	0.2
DRV_6	77°29′07″S, 162°05′54″E	1332	Dry Valleys (Mt. Peleus)	Regolith (Ferrar dolerite)	0.715740	05	11	0.715768	0.512435	10	−4.0	0.3
IH_1	73°02′25″S, 161°10′59″E	2635	Sequence Hills	Regolith (Ferrar dolerite)	0.714015	19	19	0.714043	0.512392	07	−4.8	0.2
PNTK_1	74°59′24″S, 157°55′20″E	1720	Mt. Kring	Glacial drift (beacon sandstone, Ferrar dolerite, basalt)	0.728112	19	19	0.728140	0.512026	09	−11.9	0.4

Columns 1, 2, 3: Sample code (see text), geographic coordinates of the sampling site, elevation. Columns 4, 5: Geographic area of sample provenance, typology of material collected (in brackets: parent lithologies from which the materials are inherited). Columns 6, 7, 8, 9: $^{87}Sr/^{86}Sr$ isotopic composition of samples, $\pm2\sigma_{mean} * 10^{-6}$ (internal precision, 2 standard errors of the mean), $\pm2\sigma * 10^{-6}$ (external precision). Internal precision is used if it exceeds the external (see Table 2). Normalized $^{87}Sr/^{86}Sr$ ratios from this work were corrected corresponding to a value of 0.710245 for NBS 987 standard (NBS 987 litt.0.710245; LIG 0.710217; Difference 0.000028). Columns 10, 11, 12, 13: $^{143}Nd/^{144}Nd$ isotopic composition $\pm2\sigma_{mean} * 10^{-6}$ (internal precision, 2 standard errors of the mean), Nd isotopic ratios expressed as epsilon units, uncertainty estimates based upon external precision for standard runs. Internal precision is used if it exceeds the external (see Table 2).

be well-assorted in terms of concentration and size; some consisted of typical Holocene *background* (10–25 ppb in the <5 μm size interval), others displayed either grain size larger than background, or concentration higher than average, or atypical size distribution spectrum with respect to background. A few millilitres per sample (8–27 ml, according to microparticle concentration and sample availability) were filtered in clean room (LGGE-CNRS) on polycarbonate track-etched membranes (0.4 μm porosity), taped to Al-stubs, and dedicated to SEM morphological observations and to preliminary semi-quantitative analyses of major elements through energy dispersive X-ray spectrometry (EDS).

Beside the routinely performed particle concentration and grain size analyses of laboratory MilliQ water, the control of blanks was assured by SEM visual inspection of polycarbonate membranes after filtration of about 80 ml of MilliQ laboratory water previously placed in accuvettes under artificial light conditions for 48 h.

2.4. Sr and Nd isotopic analyses

The firn core samples from Mid Point, D4, Dome C and those from the PSAs were evaporated in clean conditions (class 100 laminar flow hoods) and weighted at the Laboratory for Isotope Geology (LIG) of the Swedish Museum of Natural History. The amount of dust recovered from firn core samples was about 100–200 μg, while for PSA samples the weight spanned a broad interval from 300 μg to some mg.

All samples were digested in an acid mixture (HNO_3 + HF + $HClO_4$) and heated (60 °C) in closed vessels for 24 h. After isotopic enrichment with a mixed $^{147}Sm/^{150}Nd$ spike and a ^{84}Sr enriched spike, the solution was evaporated to dryness on a hot plate. The residue, dissolved in 4 ml 6 M HCl, was subjected to identical chemical procedures for elemental separation adopted in earlier studies and described in Delmonte et al. (2008), supplementary online material.

Isotopic analysis of Nd and Sr were performed with a Thermo Scientific TRITON TIMS. Neodymium was loaded mixed with Aquadag graphite on double rhenium filaments and run as metal in static mode using rotating gain compensation. Concentrations and ratios were reduced assuming exponential fractionation. Calculated ratios were normalised to $^{146}Nd/^{144}Nd = 0.7219$. Epsilon units are calculated as follows:

$$\varepsilon_{Nd}(0) = \left[\left(^{143}Nd/^{144}Nd\right)_{sample}/\left(^{143}Nd/^{144}Nd\right)_{CHUR} - 1\right] \times 10^4;$$
$$\times \left(\text{with } ^{143}Nd/^{144}Nd_{CHUR} = 0.512638\right)$$

External precision for $^{143}Nd/^{144}Nd$ as judged from values for 4–12 ng loads of Ndβ standard was 43 ppm. Corresponding values for >200 ng loads of La Jolla standard are 9.2 ppm and 0.5118484 ± 4.7 ($n = 32$); accuracy correction was not necessary since the mean $^{143}Nd/^{144}Nd$ ratio was 0.511895 ± 22 ($n = 20$). Purified Sr samples were mixed with tantalum activator and loaded on a single rhenium filament. Two hundred 8 s integrations were recorded in multicollector static mode, applying rotating gain compensation. Measured ^{87}Sr intensities were corrected for Rb interference assuming $^{87}Rb/^{85}Rb = 0.38600$ and ratios were reduced using the exponential fractionation law and $^{88}Sr/^{86}Sr = 8.375209$. External precision for $^{87}Sr/^{86}Sr$ as judged from running 200 ng loads of NBS SRM 987 standard is 16 ppm ($n = 33$), while loads in the range 10–50 ng results in a precision of 22 ppm ($n = 12$). Accuracy correction was applied to $^{87}Sr/^{86}Sr$ ratios corresponding to a value of 0.710245 for NBS SRM 987 standard (NBS 987: literature value 0.710245, LIG value 0.710217; Difference: 0.000028).

2.5. Present-day conditions: air mass back-trajectories calculations

In order to compare palaeo-data with present-day meteorological conditions, air mass back-trajectories were calculated with the HYSPLIT Lagrangian model (Draxler and Rolph, 2012) initialized with the ECMWF ERA INTERIM atmospheric model data Re-analysis with a 1° × 1° regular grid. Five-days back trajectories were computed daily from January 1, 1980, to December 31, 2011 (11,680 back trajectories) arriving at 12 UTC and at 500, 1000, 2000 and 4000 m over the selected sites (Dome C, D4, Mid Point and Talos Dome). No uncertainties in the resulting trajectories were calculated in this work; however an error from 10% to 30% of the travel distance after five days was estimated by Scarchilli et al. (2011) and Schlosser et al. (2008). Each trajectory was projected onto the ERA INTERIM snowfall (SF) + 12 h forecast field, in order to associate each point along the trajectory path with the SF value of the nearest model grid, assuming a constant precipitation rate within the forecasted 12 h. The frequency and pattern of dust transport from the ice-free areas of NVL and SVL towards the four selected sites during modern times was estimated selecting trajectories where air masses were lying for at least 3 h over the potential dust source areas (blue boxes in Fig. 6b) – including the northern part of Victoria Land and coastal Transantartic Mountains from the Ross Ice Shelf to the Melbourne volcano – and where no snowfall occurred since 48 h before the air mass arrival at the site, in order to disregard any wet deposition en route.

Air masses arriving 1000 m above the surface of each site were considered. Actually, trajectories arriving at 500 m above the surface of the sites are more suitable for the study of atmosphere–cryosphere interactions, but these were not taken into account because of the strong influence of the underlying model topography, especially over the steep Antarctic coast (Sinclair et al., 2010).

3. Results

3.1. Spatial variability of dust flux, size, isotopic composition

Dust concentration and size data obtained from Dome C and TD firn were compared with literature dust data respectively from EPICA-Dome C and TALDICE Holocene ice sections, to test the quality of the firn decontamination procedure adopted in this study (see supplementary information). Results were very encouraging since dust concentrations in the firn were lower than dust concentration measured in late Holocene ice samples, and the size distributions very comparable. The individual dust concentration values obtained for each firn core section are reported in the Supplementary information along with a profile of dust concentration versus depth. For each firn core under study, the mean dust concentration (calculated averaging the single values from each section) was used along with the average accumulation rate (Frezzotti et al., 2004, 2005, 2007) to calculate dust fluxes in the 1–5 μm and 5–10 μm size bins (Table 1).

The spatial variability of the average dust depositional flux against the relative distance from Talos Dome is plotted in Fig. 2a together with elevation of each drilling site and the approximate distance from the nearest rock outcrop. Aeolian microparticles having diameter between 1 and 5 μm display a marked decreasing flux along the transect, from about 0.75 (±0.35) mg m^{-2} yr^{-1} at Talos Dome and 0.50 (±0.27) mg m^{-2} yr^{-1} at Mid Point to about 0.19 (±0.13) and 0.20 (±0.14) mg m^{-2} yr^{-1} at D4 and Dome C, respectively. The values obtained for Talos Dome and Dome C on pre-industrial dust samples are in line with literature data for the same sites for the Late Holocene (0.70 and 0.33 mg m^{-2} yr^{-1} respectively, 2–5 ka B.P.) and lower than those from the Early

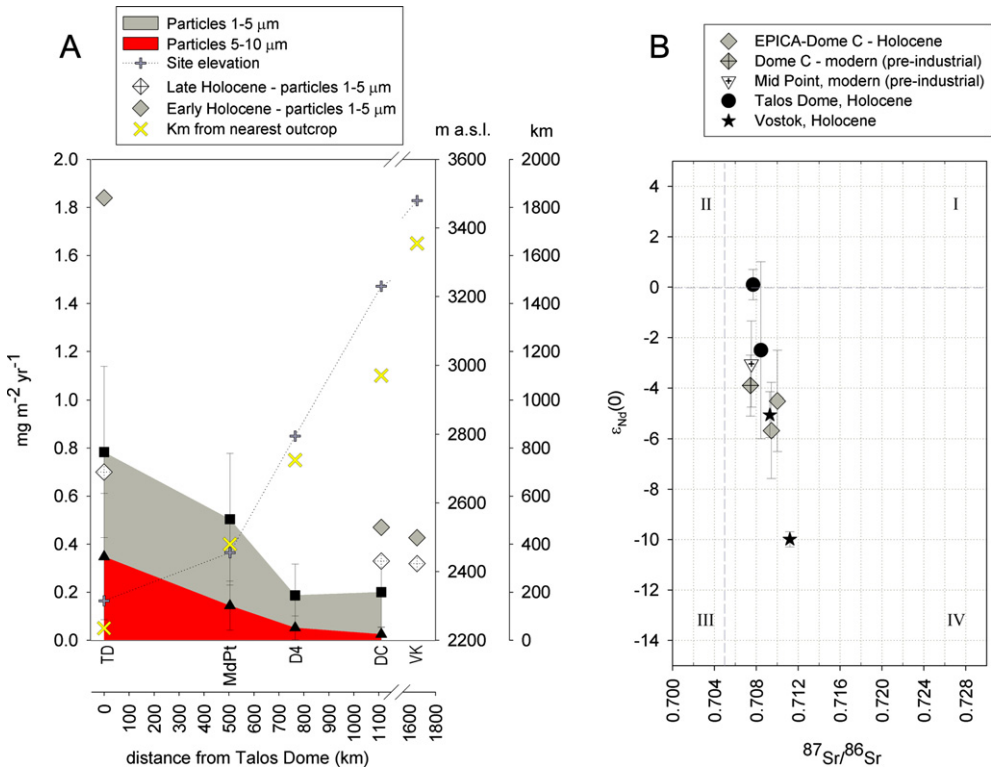

Fig. 2. Spatial variability of dust flux and isotopic composition. (A): Aeolian dust flux (mg m^{-2} yr^{-1}) at TD, MdPt, D4, DC measured on firn cores (pre-industrial samples) for particles with diameter between 1 and 5 μm (black squares) and 5–10 μm (black triangles). Dust fluxes (error bars: standard deviation of flux) are reported against the relative distance of each site from TD. For comparison, the Late Holocene (2–5 ka B.P.) and the Early Holocene (8–11.7 ka B.P.) dust flux at TALDICE (Albani et al., 2012a), Dome C and Vostok (Delmonte et al., 2005) is reported. The short-dashed line with crosses shows the topographic variability between drilling sites, the X symbol indicates the approximate distance from the nearest rock outcrop. (B): Isotopic signature ($^{87}Sr/^{86}Sr$ and $\varepsilon_{Nd}(0)$) of pre-industrial and Holocene aeolian dust in firn and ice cores from the Antarctic sector investigated in this work. MdPt and DC firn core data (pre-industrial): this work. Talos Dome (TALDICE), EPICA-DC, and Vostok ice core data (Holocene): Delmonte et al. (2007, 2010a), Basile (1997).

Holocene (1.84 and 0.47 mg m^{-2} yr^{-1} respectively, 8–11.7 ka B.P.), in agreement with the respective trends during the current interglacial (Delmonte et al., 2005; Albani et al., 2012a).

The flux of larger particles, with diameter between 5 and 10 μm, is significant only at Talos Dome (0.35 ± 0.26 mg m^{-2} yr^{-1}) and to a lesser extent at MdPt (0.14 ± 0.10 mg m^{-2} yr^{-1}), but becomes close to the detection limit at D4 and Dome C. This evidence is also in line with earlier observations on the Holocene section of the EPICA-Dome C core (Delmonte et al., 2002). In summary, with increasing distance from the periphery of the ice sheet (Talos Dome area) and with increasing elevation, our data highlight a marked decline of dust depositional flux, especially associated to a reduction of the coarse (>5 μm) size fraction.

The Sr and Nd isotopic composition of modern dust from the Mid Point, D4 and Dome C firn cores is reported in Fig. 2b and Table 2, along with the scarce literature data available from Holocene Antarctic ice core dust. The extremely low weight of the dust samples makes the 2σ (2-standard error) relatively high for $\varepsilon_{Nd}(0)$. Yet, the isotopic signature of pre-industrial dust measured in this work for Dome C is coherent with that of early and mid-Holocene dust from the EPICA-Dome C ice core (Delmonte et al., 2007).

Altogether, modern and Holocene firn and ice core dust samples from TALDICE, Mid Point, Dome C and Vostok (this work, Basile, 1997; Delmonte et al., 2007, 2010a) display $\varepsilon_{Nd}(0)$ isotopic values progressively decreasing, from the more radiogenic values of Talos Dome and Mid Point to the less radiogenic values of inner plateau. This difference between the periphery and the interior of the ice sheet is particularly evident for Nd isotopes, despite the large standard error, implying a spatial differentiation in the composition of dust during Holocene.

3.2. Microscope observations

About 50% of samples (10 over 20), among which all those displaying *typical background* characteristics, showed presence of a mixture of (1) mineral dust, (2) volcanic materials as glass shards and minerals, and (3) micrometric-sized fragments of diatoms, whose genera and species cannot be recognized because of the small dimension of the pieces. The volcanic material contained in these samples was apparently fresh, relatively unabraded and with incoherent heterogeneous composition. Four other samples did not contain volcanic material but were composed of a mixture of mineral dust and diatom fragments, as those reported in Fig. 3a and b. Two other samples showed presence of dust particles only, even larger than 5 μm in diameter, and finally, four samples consisted of primary tephra layers, whose geochemical composition and provenance are described in Narcisi et al. (2012). These primary volcanic deposits were associated to dust and diatom fragments, but this association very likely derives from sampling. Although the number of samples analyzed is too low for assessing robust statistics, we highlight that diatom fragments were observed in association with dust in the large majority of samples. Not a single fragment of microfossils was observed on the membranes where MilliQ water left under light conditions for 48 h was filtered, thus excluding the possibility of laboratory contamination.

3.3. Isotopic analyses of PSA samples

The Sr and Nd isotopic composition of the fine (<5 μm) fraction of PSA samples collected in this work is reported in Table 3 and plotted in Fig. 4 along with additional isotopic data from Victoria

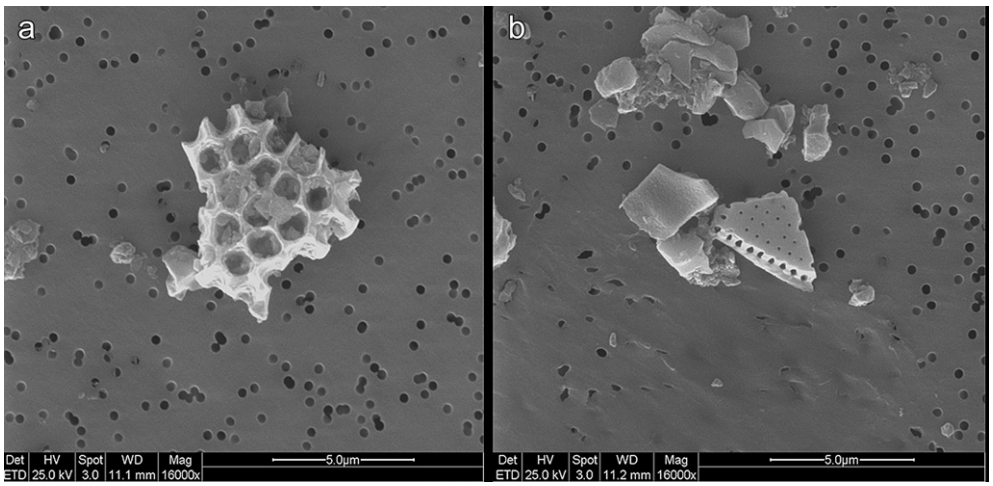

Fig. 3. SEM pictures of insoluble material from the TALDICE ice core. Coarse diatom fragments can be clearly observed in the photos (centre), surrounded by smaller lithic material. Mixture of volcanic and lithic material was observed in a good number of samples, often in association with diatom chips.

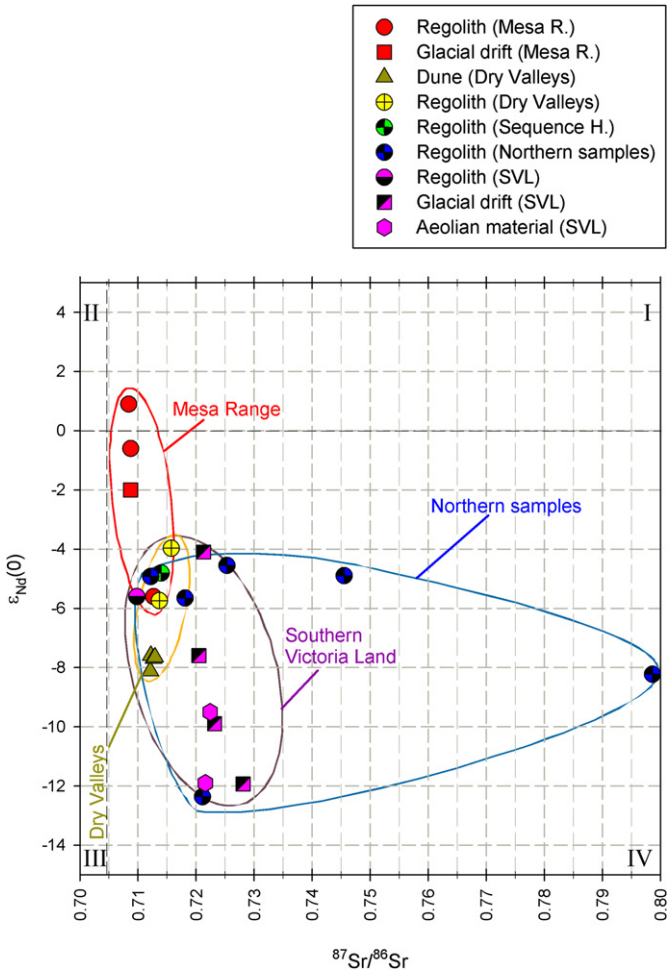

Fig. 4. Sr–Nd isotopic signature of the fine (∅ < 5 μm) fraction of PSA samples from Victoria land, grouped according to their geographic provenance. The isotopic field of samples from the Outback Nunataks northern area, from the Dry Valleys, from high-elevation sites in Southern Victoria Land and from the Mesa Range is shown. Samples consist of regolith, glacial drift, sand dunes and aeolian materials. Data source: this work and Delmonte et al. (2010a).

Land PSAs measured in an earlier study (Delmonte et al., 2010a) on the same grain size fraction. Samples are grouped according to their geographic location inside Victoria Land; as it can be observed, the samples collected N–NE from Talos Dome on the Outback Nunataks, display very scattered isotopic composition, as it can be expected from their very variable parent lithology (granite, Ferrar dolerite, Beacon sandstone, Priestley shists). The $^{87}Sr/^{86}Sr$ values span a broad interval (0.712184–0.798656) while $\varepsilon_{Nd}(0)$ displays low radiogenic values (−4.5 to −12.4). Sand dune samples from the Dry Valleys, on the opposite, display very clustered isotopic composition, because of the high degree of mixing of these materials and the uniform parent lithology (Beacon sandstone). All samples from Dry Valleys, including those collected at high altitude on Mt. Gran and Mt. Peleus (Ferrar dolerites) are included in the isotopic field of sediments from Southern Victoria Land. This latter field was constructed on the basis of isotopic data from regolith, glacial drifts and aeolian materials collected on the topmost part of Ricker Hills, The Mitten and Griffin Nunataks measured on the same size fraction (Delmonte et al., 2010a) plus an additional glacial drift sample from Mount Kring measured in this work. All these SVL samples are derived from a mixture of Beacon sandstone, Ferrar dolerites and Kirkpatrick basalts.

The Mesa Range group includes regolith and glacial deposits from the area of the Mesas, among which samples from Tobin and Pain Mesa (Ferrar dolerites) and Chisholm Hills (Beacon sandstone). The characteristics of these samples were described in Delmonte et al. (2010a). Also, isotopic data of one regolith from Sequence Hills (Ferrar dolerites), a site belonging to the group of intermediate hills between the Mesas and the Outback Nunataks, are reported.

Clearly a better clustering of data can be obtained grouping samples according to their parent materials, as shown in Fig. 5. The isotopic field of regolith and drifts developed on granite occupies an area in quadrant IV that is markedly secluded from the others because of the very radiogenic $^{87}Sr/^{86}Sr$ isotopic composition of samples. The remaining groups consist of materials deriving from (1) Ferrar dolerite, (2) Beacon sandstone, and from (3) a mixture of Ferrar dolerite, Beacon sandstone, Kirkpatrick basalts plus in some cases a possible additional contribution from SVL granites. Significant differences among these groups, based on comparing the Sr and Nd isotopic values separately, are suggested by a Kruskal–Wallis test (a nonparametric test that compares three or more unpaired groups). A pairwise comparison (Dunn's test, $P = 0.05$)

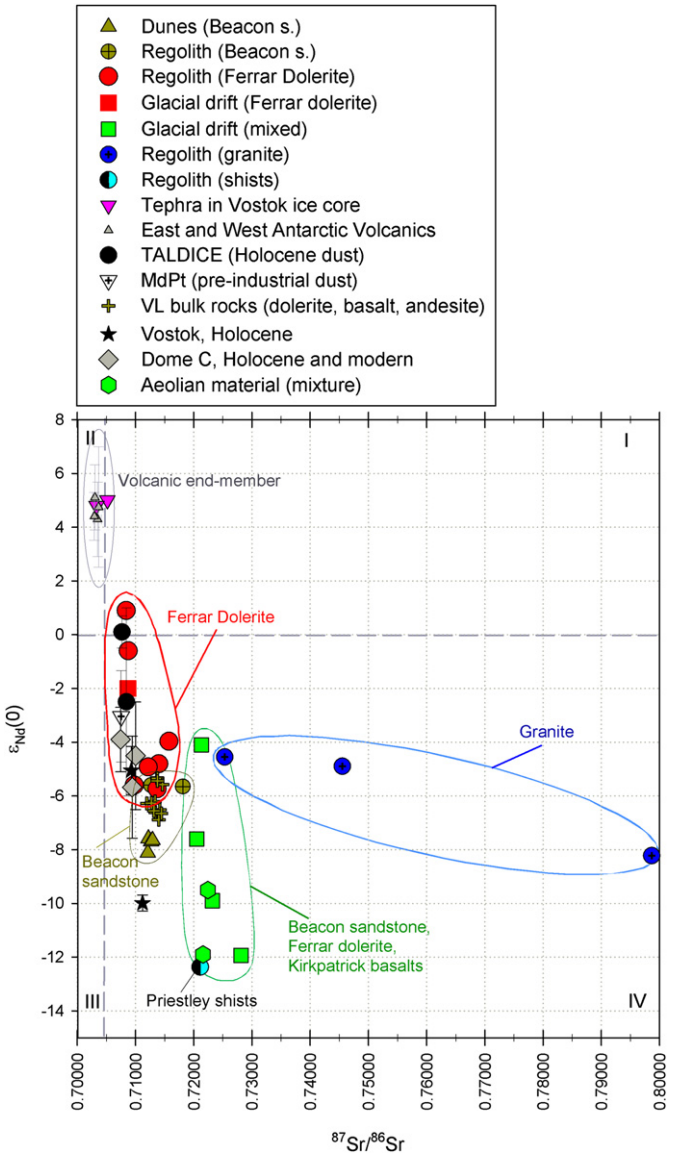

Fig. 5. Isotopic signature of Holocene and modern ice and firn core dust and dust-sized fraction of Victoria land PSA samples differentiated according to the lithology of parent materials (data source: this work, Delmonte et al., 2010a). Vertical bars for core data correspond to 2-standard error for Nd; the volcanic end-member has been plotted on the basis of the isotopic composition of East and West Antarctic volcanic rocks (GEOROC database: http://georoc.mpch-mainz.gwdg.de/georoc/) along with the isotopic composition of two Antarctic tephra layers from the Vostok ice core (Basile et al., 2001). Whole-rock data from dolerites, basalts and andesites from the Victoria Land (Mesa Range and Prince Albert Mountains) are also reported for comparison (Elliot et al., 1995; Fleming et al., 1995; Antonini et al., 1999; Faure and Mensing, 2010 and references therein; GEOROC database: http://georoc.mpch-mainz.gwdg.de/georoc/).

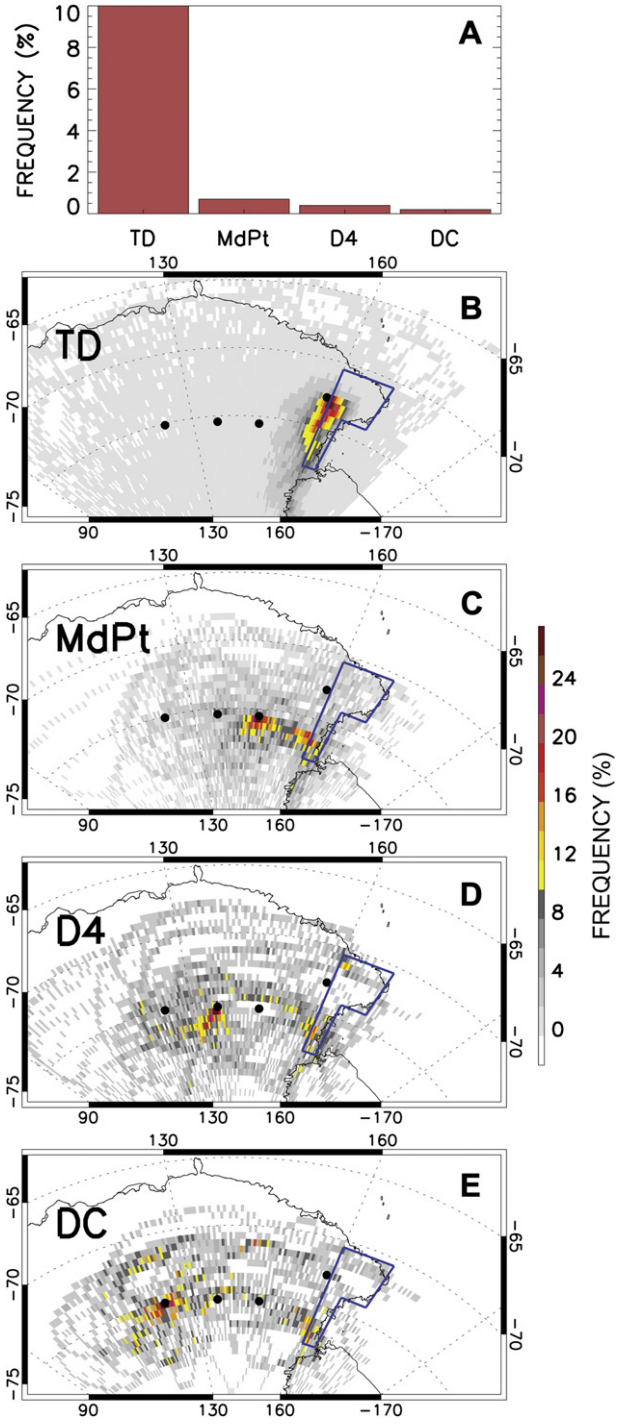

Fig. 6. Potential dust-carrying events derived from back trajectory calculations. (A) Frequency (%) of 5-days back trajectories lying for at least 3 h over the potential dust source areas (blue boxes in B–E) and arriving at 1000 m above surface at Talos Dome (TD), Mid Point (MdPt), D4 and Dome C (DC) without snowfall over the preceding 48 h. (B–E) Frequency (filled contour, %) of number of back trajectories, fulfilling the conditions mentioned in A, lying over each 0.5° × 0.5° area and connecting the potential dust source areas (blue boxes) to the sites of TD, MdPt, D4 and DC, respectively. (For interpretation of the references to colour in this figure legend, the reader is referred to the web version of this article.)

reveals that group 1 (Ferrar dolerites) and group 3 (Mixed dolerites, basalts and Beacon sandstone) are significantly different for both Sr and Nd isotopes, while group 2 (Beacon Sandstone) and group 3 (Mixture) differ significantly only for their Sr isotopic composition.

3.4. Air mass pathways connecting PSAs and drilling sites at present-day

Results from back trajectory calculations are reported in Fig. 6a and b. About 10% of the trajectories reaching Talos Dome at present-day (1980–2011 A.D.) are potentially suitable for local dust advection to the site, i.e. have been lying for at least 3 h above the PSAs and reach the site 1000 m above surface without snow precipitation over the preceding 48 h. Conversely, for the more inner sites of Mid Point, D4 and Dome C, the frequency of trajectories fulfilling the above-mentioned conditions is extremely low, around

0.7%, 0.4% and 0.2% respectively (Fig. 6a). It must be mentioned that all the four studied sites are strongly influenced by katabatic wind blowing from highest part of the plateau towards the coast for the most part of the time. Seasonality analysis reveals that in the case of Talos Dome, these trajectories mostly occur during spring and summer seasons. Furthermore, the air mass pathways connecting source areas to this site are mainly driven by the local atmospheric circulation in the Ross Sea area, and mostly flow parallel to the Victoria Land coast along an S–N direction (Fig. 6b). No significant differences can be observed between prevailing surface wind provenance (200°–160°) and direction of potential dust-transporting events for the site of Talos Dome. For the other sites, conversely, the extremely rare occurrence of these potentially dust-carrying events does not allow creating a robust statistics, and the transport patterns to inner sites seem to be more connected to strong random events than to seasonal features. On the whole, air mass intrusions towards the interior seem to occur over the area between the Ross Ice Shelf and the Drygalski Ice Tongue. In any case, these potential dust carrying events are connected to a shift of about 90° from the main wind direction (180°–240°).

Among trajectories potentially suitable for local dust transport, those reaching Talos Dome lie on average at lower altitude over the potential source areas (ca 800 m above surface) with respect to trajectories reaching internal sites (1300, 1180, 1140 m for MdPt, D4 and DC, respectively), but these estimates are affected by a high degree of variability – up to 75% of mean value.

4. Discussion

4.1. Dust variability from the periphery to the interior of the ice sheet

The depositional flux of aeolian mineral dust displays a marked decrease with increasing distance from the margin of the ice sheet (Talos Dome area) and with increasing altitude. For the pre-industrial (1400 A.D.–1800 A.D.) samples analyzed, the average flux of typical Aeolian dust particles having diameter smaller than 5 μm is about 4 times higher at Talos Dome with respect to Dome C. A similar flux ratio was calculated for the Early Holocene (8–11.7 ka B.P.) between TD and DC (about 4) and between TD and VK (about 4.4), while for the Late Holocene (2–5 ka B.P.) it was about 2 times higher at TD with respect to DC and VK.

Larger dust particles (5 μm $< \varnothing <$ 10 μm) clearly represent a non-negligible contribution to the total dust input only at Talos Dome and to a lesser extent at Mid Point, while they are almost absent at D4 and Dome C. This is noteworthy, as in the inner part of the Antarctic plateau such large particles were exclusively observed in association with tephra layers (Basile et al., 2001; Narcisi et al., 2005), or with spurious counts caused by analytical noise and/or contamination of samples (Delmonte et al., 2002). The spatial variability of dust flux allows making a differentiation between typical high-altitude plateau sites (Dome C and D4), where the extremely low dust fluxes are representative of the pristine natural background of inner East Antarctica for the centuries preceding the industrial revolution, and the peripheral site of Talos Dome, MdPt displaying intermediate characteristics. Also, the isotopic composition of Holocene and pre-industrial mineral dust extracted from plateau and from peripheral ice and firn cores highlights a similar differentiation. Whilst $^{87}Sr/^{86}Sr$ ratios are very similar, the $\varepsilon_{Nd}(0)$ values display a tendency from more radiogenic to less radiogenic values when going from Talos Dome and Mid Point to Dome C and Vostok. As the Nd isotopic composition of mineral dust is strongly related to dust origin (e.g. Feng et al., 2009), the gradient observed can be ascribed to a different dust composition from the periphery to the interior of the ice sheet. The spatial gradient of dust flux and the related variation of isotopic fingerprint can be reasonably explained in terms of a different influence from local dust sources with increasing distance from the ice-free terrains of the Transantarctic Mountains and with increasing elevation. However these are not the only factors involved, as this feature can be associated also to different atmospheric circulation regimes at Talos Dome and on the inner polar plateau (Section 4.4).

All these evidences between peripheral sites as Talos Dome and plateau sites as D4 and DC are in line with evidences from former studies (Proposito et al., 2002; Magand et al., 2004), where a drastic decrease in concentration of primary aerosol components was observed with increasing altitude and distance from the coast, in parallel with lower accumulation rates and temperatures, with typical plateau conditions fully established between Mid Point and D4.

4.2. Microscope observations

Electron microscope morphological observations on Holocene ice core dust samples from Talos Dome provide fundamental support for data interpretation. Important evidences sustaining the hypothesis of a proximal origin for dust at the site are represented by the presence of large particles with high settling velocity and by micrometric-sized diatom fragments. It is well known that diatom frustles, which are light and easily carried by winds, represent a small but pervasive component of Antarctic sediments even at high elevation sites (>2000 m a.s.l., McKay et al., 2008). These micro-organisms can be windborne to and on the Antarctic polar ice cap (Burckle et al., 1997), occasionally reaching internal sites such as South Pole (Kellogg and Kellogg, 1996). According to Burckle and Delaney (1999), the entrainment of microfossils (diatom clasts, sponge spicules, opal phytoliths) along with dust in rock cracks is a very common process in Antarctica. Burckle et al. (1997) also proposed a mechanism for the emplacement and concentration of diatom clasts in glacial deposits, and for their possible recycling. In the specific case of Talos Dome, the small size of the fragments suggests reworking from subaerially exposed sediments. Yet, post-depositional comminution related to glacial compression after diatom trapping and burying in snow layers cannot be excluded *a priori*. Although atmospheric circulation may allow sampling of windborne material from large portions of the Southern hemisphere and transport to Antarctica, the very common presence of diatom fragments in Antarctic sediments and in the Antarctic atmosphere in proximity of the Transantarctic Mountains (McKay et al., 2008) strongly points towards a transport processes from local sources.

Microscopic observations also highlighted presence of abundant volcanic material in the samples, including those that are representative of *background* environmental conditions at the site. The characteristics of the volcanic particles as well as their geochemical heterogeneity suggest these represent an intrinsic component of the environmental background mineral aerosol in the area. The characteristics of this volcanic component, incompatible with derivation from a primary volcanic eruption, suggest a remobilization of volcanic particles from different volcanic sources. The presence of a persistent volcanic component in the samples, even in low-concentrated ones, is also very important for the interpretation of isotopic data, as discussed below. We note that Holocene samples from Talos Dome also revealed anomalously high magnetization, pointing towards a volcanic contribution to this highly magnetic dust (Lanci and Delmonte, in press). The importance of the volcanic contribution was already inferred for the Holocene on the basis of trace elements and lead isotope data from various drilling sites in Victoria Land (Van de Velde et al., 2005) and from the Taylor Dome ice core (Matsumoto and Hinkley, 2001), where volcanic fallout is

mostly in gaseous or condensed form. For Vostok and Dome C, conversely, a volcanic contribution to the total Pb content was observed but it seems quantitatively minor (Hong et al., 2003; Vallelonga et al., 2005, 2010). Ice and firn layers can incorporate together the gaseous and the solid silicate (tephra) components of volcanic plumes. While gas-derived aerosol fallout recorded in polar ice can be used for instance to document interactions between volcanism and climate changes (e.g. Castellano et al., 2004), insoluble tephra layers derived from primary volcanic eruptions can be fundamental for chronostratigraphic correlation and can contribute significantly to paleoclimate interpretations (e.g. Narcisi et al., 2005). In the case of Talos Dome, where several primary volcanic tephras have also been detected (Narcisi et al., 2012), we highlight in this work the recurrent occurrence of geochemically heterogeneous volcanic particles, that represent a fraction of the total insoluble aerosol flux to the site and likely derive from deflation of different volcanic sources located along the air mass pathways. In this scenario, these heterogeneous volcanic particles underwent two processes: first, atmospheric injection during the primary eruption, transport governed by the atmospheric conditions at the time of the volcanic event and deposition, and successively a "recycling" associated to wind remobilization of the small volcanic particles from the area(s) of primary deposition, following the same dynamics of Aeolian dust transport and deposition to the ice core drilling site.

4.3. Dust sources in Victoria Land

On the periphery of the East Antarctic ice sheet, sizeable ice and snow free areas occur both at low altitude, particularly in coastal regions, and at high altitude even above 3000 m a.s.l. Many of these outcrops were ice-free since millions of years (e.g. Oberholzer et al., 2008; Strasky et al., 2009) and were subject to physical and chemical weathering processes leading in some cases to the formation of soil or regolith (Tedrow and Ugolini, 1966). The fine, loose sediments deriving from alteration of exposed surfaces represent primary sources for mineral dust potentially available for aeolian deflation and transport, together with unconsolidated Pleistocene glacial deposits.

In general, the Sr–Nd isotopic composition of dust and sediments is primarily related to lithology and geologic age of parent materials (Faure, 1986), although the Sr isotopic composition may be influenced by dust grain size, when diameters in the interval between 2 and 50 μm are considered (Feng et al., 2009, and references therein). The samples analyzed in this work were size-selected ($\varnothing < 5$ μm) in order to be comparable to ice core dust and in coherency with similar studies in Antarctica. Therefore, the size-dependent Sr isotopic fractionation can be neglected in this case.

When data are grouped according to the geographic origin of the sediments (Fig. 4) the data scattering becomes important and isotopic fields overlap. Scattering is more pronounced when parent lithologies from which the materials are inherited are more heterogeneous inside the group, and when the degree of mixing of the deposits is low. As an example, the high degree of scattering associated to the isotopic field of the Northern samples from the Outback Nunataks can be related to the lithological heterogeneity and to the low degree of mixing of samples, consisting of regolith developed on Ferrar dolerite, on granite, on shist and on metamorphosed Beacon sandstone as well as glacial deposits from granite. Conversely, the much clustered isotopic composition of the dunes located within the Dry Valleys is related to the intrinsic nature of these deposits, subjected to intense aeolian reworking and transport, and likely inherited from Beacon sandstone units.

Isotopic data on the dust fraction of sediments appears much more homogeneous when considering the parent rocks from which the materials are derived (Fig. 5); this is also related to their low degree of chemical weathering. In this respect, we clearly distinguish granitic materials, very radiogenic in Sr, from those derived from Ferrar dolerite, Beacon sandstone, and from a mixture of different lithologies such as Ferrar dolerite, Beacon sandstone and Kirkpatrick basalt. As it can be observed in Fig. 5, the isotopic fingerprint of small-sized dust samples is coherent at first order with literature data from whole-rock dolerites, andesites and basalts from the Mesa Range and Prince Albert Mountain areas (Elliot et al., 1995; Fleming et al., 1995; Antonini et al., 1999; GEOROC database: http://georoc.mpch-mainz.gwdg.de/georoc/; Faure and Mensing, 2010 and references therein).

A comparison of Victoria Land PSA and Holocene/modern ice and firn core dust samples is reported in Fig. 5. For Talos Dome, where a local contribution is apparent, data interpretation is complicated by the ubiquitous mixing of volcanic particles with continental dust *sensu stricto* in the background mineral samples. Therefore, although aeolian dust samples are remarkably similar to Ferrar dolerite, the influence of the volcanic pole on the geochemical signature of the samples prevents a clear discrimination of the other end-members. This is a first important limitation to the identification of a local sub-region. Also, it is well known that the composition of a dust plume can evolve along the pathway of air masses when these lie over different substrates; therefore, the geochemical composition at the deposition site represents the final result of aeolian deflation from different terrains. Finally, an additional dust input from one or more remote sources is also likely, but this latter cannot be discriminated with isotopic techniques because of the volcanic and local contributions. Despite these limitations, the PSA isotopic data obtained in this work represent an essential step forward towards the documentation of northern and southern Victoria Land dust fingerprint, which can be very useful for tracking dust provenance in many areas of the ice sheet.

We note also that the isotopic composition of Holocene and modern dust from Dome C is consistent with the isotopic signature of Antarctic Ferrar Dolerites and Beacon sandstone, and compatible with a mixture of these latter with a minor volcanic component. Although this intriguing geochemical similarity points towards a possible contribution of Antarctic dust to Dome C during Holocene, caution must be taken in this comparison since a mixed Australian and South American dust provenance to these inner sites is expected on the basis of other geochemical evidences (Revel-Rolland et al., 2006; Delmonte et al., 2007; Marino et al., 2008; De Deckker et al., 2010; Gabrielli et al., 2010) and atmospheric general circulation models (e.g. Krinner et al., 2010 and references therein). Also, as remarked inSection 3.4, the exceptionally low frequency of back trajectories lying over the potential dust source areas and arriving at low altitude above inner plateau sites suggests that low-level air mass advections enhanced by cyclonic systems are extremely unlikely for Dome C. For this site and in general for the interior of the Antarctic plateau, dust advection likely occurs via air mass convergence in the middle-high troposphere above Antarctica (Li et al., 2008; Krinner et al., 2010). Therefore, at this stage no definite conclusions can be drawn for inner sites concerning candidate end-members. In this respect, a more comprehensive comparison including local and remote sources is demanded.

4.4. Dust-related information from inner and from peripheral Antarctic ice cores

The most well-known information obtained from long ice core dust sequences coming from the interior of the East Antarctic ice sheet comes from their capability to reconstruct past atmospheric circulation changes on a hemispheric to global scale, environmental conditions at the dust source areas, and the efficiency of aerosol

transport to the polar regions, that is related to the hydrological cycle (Yung et al., 1996; Petit et al., 1999). The coupling between dust and climate on glacial/interglacial timescale has been studied in detail from the EPICA-Dome C (EDC) and from the Vostok deep ice cores (Lambert et al., 2008; Petit and Delmonte, 2009). The large (a factor about 50) dust concentration changes occurring during the major glacial/interglacial climate changes were largely attributed to synergetic changes in accumulation rate in Antarctica, source productivity and dust atmospheric life-time, all factors related to temperature and to the hydrological cycle. During the Last Glacial Maximum and the early deglaciation the westerly circulation regime allowed an efficient dust transfer from southern South America to most of the East Antarctic plateau (Basile et al., 1997; Marino et al., 2009; Delmonte et al., 2010b), and the depositional flux of mineral particles was fairly uniform (Albani et al., 2012b). During the current interglacial, conversely, different areas of the East Antarctic plateau show site-specific dust characteristics, as well as a marked compositional variability throughout the Holocene, that point towards a possible variable contribution from multiple remote sources, perhaps South America and Australia (Basile et al., 1997; Delmonte et al., 2007; Gabrielli et al., 2010; Vallelonga et al., 2010; Wegner et al., 2012). Model-based attempts to quantify the contribution of the major Southern Hemisphere sources in Antarctica (Li et al., 2008; Albani et al., 2012b) revealed that dust depositing in central East Antarctica (Dome C and Vostok area) in modern times comes from South America and Australia in comparable amounts, in agreement with the conclusions of Revel-Rolland et al. (2006).

For the area of Talos Dome, the modelled contribution of each source to the dust mass burden and deposition shows an important contribution from Australia, but neither Antarctic local sources nor volcanic material is taken into account by models (Li et al., 2008; Albani et al., 2012b). Analyses of back-trajectories carried out in this work show that aeolian drift of mineral dust from high-elevation sources of Victoria Land towards Talos Dome is not a rare event, and that it is mostly associated to mesoscale atmospheric processes leading to northward air mass flow in Victoria Land over the Prince Albert Mountains-Deep Freeze Range and Mesa Range. Therefore, it is not only the altitude of the sites and distance from the exposed source areas that modulates the importance of local dust transport but also the regional atmospheric circulation regime. The air flow pattern identified for present-day conditions likely resembles the scenario in the time period between the 15th and the 19th centuries spanned by the firn core samples. In fact, this time frame includes the Little Ice Age, for which only local variations were observed in the western Ross Sea and Victoria Land (Baroni and Orombelli, 1994; Hall, 2009). In earlier Holocene times, conversely, the regional air mass circulation patterns were likely different, in relation to the varying sea ice conditions in the Ross Sea (Hall et al., 2006) which is known to influence the mesoscale atmospheric circulation in the area (Albani et al., 2012a), as also suggested by chemical data (Becagli et al., 2004; Traversi et al., 2004).

The Ross Sea sector of East Antarctica is an area of intense mesoscale cyclogenesis, even in dry form (Carrasco et al., 2003) which is more favourable for dust transport inland. It is very likely, therefore, that dust mobilization from exposed terrains of the Transantarctic Mountains and transport to the peripheral regions of the ice sheet is a common phenomenon both today and in the past. However, the regional atmospheric circulation patterns probably changed through time as consequence of the retreat of the Ross Ice Shelf and the opening of the Ross Sea embayment (Albani et al., 2012a), and from a spatial perspective the areas involved by aeolian deflation inside Victoria Land may have changed in time. However, the marked difference in dust flux between Talos Dome and Dome C during the whole Holocene (Albani et al., 2012a) suggest that the spatial gradients of dust flux observed in this work for modern times were likely present all through the current interglacial, and were probably more pronounced after deglaciation in early Holocene times.

From a palaeoclimatic perspective, this work highlights that climate and environmental information which can be extracted from palaeo-dust records from the Antarctic ice sheet can be significantly different according to the origin of dust and transport processes involved. Actually, dust analysis in ice cores acquires specific significance for palaeoclimatic reconstruction when the geomorphological setting and the surface exposure age of potential sources are defined. While dust records from high elevation plateau sites from central East Antarctica undoubtedly reflect the environmental and climate history of large portions of the Southern hemisphere and are sensitive to long-range atmospheric transport conditions to Antarctica, the dust history at marginal sites located in proximity of the Transantarctic Mountains afford insights into regional atmospheric circulation and sea ice behaviour under conditions that, at times, may have been significantly different than present.

5. Conclusions

A marked decrease of dust flux and grain size, along with a changing isotopic composition, have been observed along a transect from Talos Dome to the higher, internal plateau sites (Dome C and Vostok area) on the basis of firn core data spanning the pre-industrial period from the 15th to the 19th century. Such a spatial variability has been associated to a different provenance of the aeolian dust on a regional scale, and in particular to an important contribution of particles from Antarctic high-elevation sources to the marginal site of Talos Dome and to a lesser extent at Mid Point, but absent in central plateau areas. Particle supply from proximal sources is also suggested by the presence of small diatom fragments – a typical characteristic of Antarctic sediments – in the Talos Dome ice core all through the Holocene part of the core. Comparison with Holocene data suggests that spatial gradients of dust flux were present all over the Holocene.

The isotopic composition of high-elevation potential source areas from Victoria Land documented in this work and in literature appears closely related to the parent lithology of the materials; however, the pervasive presence of volcanic particles representing a typical feature of background aerosol at Talos Dome prevents a direct comparison of isotopic fingerprints. For present-day conditions and likely for the pre-industrial period investigated, the frequency of air mass trajectories potentially suitable for local dust transport to Talos Dome is moderately high, and displays a well-defined seasonality (spring/summer) and spatial pattern, this latter following southerly flow directed northward alongside the Transantarctic Mountains. Conversely, for all the other sites investigated the occurrence of potential dust-carrying events seem extremely uncommon.

Peripheral ice sheet locations close to ice-free areas are thus important for an improved characterization of the dust cycle in polar areas, and for a deeper understanding of interactions between atmospheric circulation and aeolian dust transport, which is relevant to palaeoclimate reconstructions.

Acknowledgements

This work was supported by SYNTHESYS funding (project SE-TAF-212) made available by the European Community under the FP7. The Talos Dome Ice core Project (TALDICE), a joint European programme, is funded by national contributions from Italy, France,

Germany, Switzerland and the United Kingdom. Main logistic support was provided by PNRA. This is TALDICE publication no. 28.

This work is a contribution to PRIN 2009 research project "Variability and geographic provenance of eolian dust in Antarctica during the late Quaternary: a multi-parametric approach with the use of cutting-edge techniques" and to HOLOCLIP Project, a joint research project of ESF PolarCLIMATE programme, funded by national contributions from Italy, France, Germany, Spain, Netherlands, Belgium and the United Kingdom.

In Italy HOLOCLIP is funded by PNRA. This is HOLOCLIP publication no. 14.

Many thanks to Dr. Paul Augustinus, School of Geography, Geology and Environmental Science, University of Auckland, New Zealand who very kindly supplied samples from dunes in the Dry Valleys.

The authors gratefully acknowledge the NOAA Air Resources Laboratory (ARL) for the provision of the HYSPLIT transport and dispersion model used in this publication.

Appendix A. Supplementary material

Supplementary material associated with this article can be found, in the online version, at http://dx.doi.org/10.1016/j.quascirev.2012.11.033.

References

Albani, S., Delmonte, B., Maggi, V., Baroni, C., Petit, J.R., Stenni, B., Mazzola, C., Frezzotti, M., 2012a. Interpreting last glacial to Holocene dust changes at Talos Dome (East Antarctica): implications for atmospheric variations from regional to hemispheric scales. Climate of the Past 8 (2), 741–750. http://dx.doi.org/10.5194/cp-8-741-2012.

Albani, S., Mahowald, N.M., Delmonte, B., Maggi, V., Winckler, G., 2012b. Comparing modeled and observed changes in mineral dust transport and deposition to Antarctica between the Last Glacial Maximum and current climates. Climate Dynamics 38 (9–10), 1731–1755. http://dx.doi.org/10.1007/s00382-011-1139-5.

Antonini, P., Piccirillo, E.M., Petrini, R., Civetta, L., D'Antonio, M., Orsi, G., 1999. Enriched mantle – Dupal signature in the genesis of the Jurassic Ferrar tholeiites from Prince Albert Mountains (Victoria Land, Antarctica). Contributions to Mineralogy and Petrology 136, 1–19.

Armienti, P., Baroni, C., 1999. Cenozoic climatic change in Antarctica recorded by volcanic activity and landscape evolution. Geology 27 (7), 617–620.

Baroni, C., Orombelli, G., 1994. Holocene glacier variations in the Terra Nova Bay area (Victoria Land, Antarctica). Antarctic Science 6 (4), 497–505.

Baroni, C., Fasano, F., Giorgetti, G., Salvatore, M.C., Ribecai, C., 2008. The Ricker Hills Tillite provides evidence of Oligocene warm-based glaciation in Victoria Land, Antarctica. Global and Planetary Change 60 (3–4), 457–470.

Baroni, C., Frezzotti, M., Salvatore, M.C., Meneghel, M., Tabacco, I.E., Vittuari, L., Bondesan, A., Biasini, A., Cimbelli, A., Orombelli, G., 2004. Antarctic geomorphological and glaciological 1:250 000 map series: Mount Murchison quadrangle, northern Victoria Land. Explanatory notes. Annals of Glaciology 39, 256–264.

Baroni, C., Noti, V., Ciccacci, S., Righini, G., Salvatore, M.C., 2005. Fluvial origin of the valley system in northern Victoria Land (Antarctica) from quantitative geomorphic analysis. Bulletin of the Geological Society of America 117 (1–2), 212–228.

Basile, I., Grousset, F.E., Revel, M., Petit, J.R., Biscaye, P.E., Barkov, N.I., 1997. Patagonian origin of glacial dust deposited in East Antarctica (Vostok and Dome C) during glacial stages 2, 4 and 6. Earth and Planetary Science Letters 146, 573–589.

Basile, I., 1997. Origine des aerosols volcaniques et continentaux de la carotte de glace de Vostok (Antarctique). PhD thesis, Université J. Fourier Grenoble-I.

Basile, I., Petit, J.R., Touron, S., Grousset, F.E., Barkov, N., 2001. Volcanic layers in Antarctic (Vostok) ice cores: source identification and atmospheric implications. Journal of Geophysical Research 106 (D23), 31915–31931.

Becagli, S., Proposito, M., Benassai, S., Flora, O., Genoni, L., Gragnani, R., Largiuni, O., Pili, S.L., Severi, M., Stenni, B., Traversi, R., Udisti, R., Frezzotti, M., 2004. Chemical and isotopic snow variability in East Antarctica along the 2001/02 ITASE traverse. Annals of Glaciology 39, 473–482.

Bory, A., Wolff, E., Mulvaney, R., Jagoutz, E., Wegner, A., Ruth, U., Elderfield, H., 2010. Multiple sources supply eolian mineral dust to the Atlantic sector of coastal Antarctica: evidence from recent snow layers at the top of Berkner Island ice sheet. Earth and Planetary Science Letters 291, 138–148.

Bristow, C.S., Jol, H.M., Augustinus, P., Wallis, I., 2010a. Slipfaceless 'whaleback' dunes in a polar desert, Victoria Valley, Antarctica: insights from ground penetrating radar. Geomorphology 114, 361–372.

Bristow, C.S., Augustinus, P.C., Wallis, I.C., Jol, H.M., Rhodes, E.J., 2010b. Investigation of the age and migration of reversing dunes in Antarctica using GPR and OSL, with implications for GPR on Mars. Earth and Planetary Science Letters 289, 30–42.

Bristow, C.S., Augustinus, P., Rhodes, E.J., Wallis, I.C., Jol, H.M., 2011. Is climate change affecting rates of dune migration in Antarctica? Geology 39, 831–834. http://dx.doi.org/10.1130/G32212.1.

Buiron, D., Chappellaz, J., Stenni, B., Frezzotti, M., Baumgartner, M., Capron, E., Landais, A., Le mieux-Dudon, B., Masson-Delmotte, V., Montagnat, M., Parrenin, F., Schilt, A., 2011. TALDICE-1 age scale of the Talos Dome deep ice core, East Antarctica. Climate of the Past 7, 1–16. http://dx.doi.org/10.5194/cp-7-1-2011.

Burckle, L.H., Delaney, J.S., 1999. Terrestrial microfossils in Antarctic ordinary chondrites. Meteoritics & Planetary Science 34 (3), 475–478.

Burckle, L.H., Kellogg, D.A., Kellogg, T.B., Fastook, J.L., 1997. A mechanism for emplacement and concentrations of diatoms in glacigenic deposits. Boreas 26, 55–60.

Calkin, P.E., Rutford, R.H., 1974. The sand dunes of Victoria Valley, Antarctica. Geographical Review 64 (2), 189–216.

Carrasco, J.F., Bromwich, D.H., Monaghan, A.J., 2003. Distribution and characteristics of mesoscale cyclones in the Antarctic: Ross Seas Eastward to the Weddell Sea. Monthly Weather Review 131, 289–301.

Castellano, E., Becagli, S., Jouzel, J., Migliori, A., Severi, M., Steffensen, J.P., Traversi, R., Udisti, R., 2004. Volcanic eruption frequency over the last 45 ky as recorded in EPICA-Dome C ice core (East Antarctica) and its relationship with climatic changes. Global and Planetary Change 42, 195–205.

De Deckker, P., Norman, M., Goodwin, I.D., Wain, A., Gingele, F.X., 2010. Lead isotopic evidence for an Australian source of aeolian dust to Antarctica at times over the last 170,000 years. Palaeogeography, Palaeoclimatology, Palaeoecology 285 (3–4), 205–223. http://dx.doi.org/10.1016/j.palaeo.2009.11.013.

Delmonte, B., Petit, J.R., Maggi, V., 2002. Glacial to Holocene implications of the new 27,000 year dust record from the EPICA Dome C (East Antarctica) ice core. Climate Dynamics 18 (8), 647–660. http://dx.doi.org/10.1007/s00382-001-0193-9.

Delmonte, B., Petit, J.R., Krinner, G., Maggi, V., Jouzel, J., Udisti, R., 2005. Ice core evidence for secular variability and 200-year dipolar oscillations in atmospheric circulation over East Antarctica during the Holocene. Climate Dynamics 24, 641–654. http://dx.doi.org/10.1007/s00382-005-0012-9.

Delmonte, B., Petit, J.R., Basile-Doelsch, I., Jagoutz, E., Maggi, V., 2007. Late Quaternary Interglacials in East Antarctica from ice core dust records. In: Sirocko, F., Claussen, M., Sánchez Goni, M.F., Litt, Th (Eds.), The Climate of Past Interglacials. In: Van der Meer, J.J.M. (Ed.),, Developments in Quaternary Science, vol 7. Springer, pp. 53–73.

Delmonte, B., Andersson, P.S., Hansson, M., Schoberg, H., Petit, J.R., Basile-Doelsch, I., Maggi, V., 2008. Aeolian dust in East Antarctica (EPICA-Dome C and Vostok): provenance during glacial ages over the last 800 ka. Geophysical Research Letters 35, L07703.

Delmonte, B., Baroni, C., Andersson, P.S., Schoberg, H., Hansson, M., Aciego, S., Petit, J.R., Albani, S., Mazzola, C., Maggi, V., Frezzotti, M., 2010a. Aeolian dust in the Talos Dome ice core (East Antarctica, Pacific/Ross Sea sector): Victoria Land versus remote sources over the last two climate cycles. Journal of Quaternary Science 25 (8), 1327–1337. http://dx.doi.org/10.1002/jqs.1418.

Delmonte, B., Andersson, P.S., Schoberg, H., Hansson, M., Petit, J.R., Delmas, R., Gaiero, D.M., Maggi, V., Frezzotti, M., 2010b. Geographic provenance of aeolian dust in East Antarctica during Pleistocene glaciations: preliminary results from Talos Dome and comparison with East Antarctic and new Andean ice core data. Quaternary Science Reviews 29 (1–2), 256–264. http://dx.doi.org/10.1016/j.quascirev.2009.05.010.

Deines, P., Goldstein, S.L., Oelkers, E.H., Rudnick, R.L., Walter, L.M., 15 December 2003. Standards for publication of isotope ratio and chemical data in Chemical Geology. Chemical Geology 202 (1–2), 1–4. http://dx.doi.org/10.1016/j.chemgeo.2003.08.003.

Di Nicola, L., Strasky, S., Schlüchter, C., Salvatore, M.C., Akçar, N., Kubik, P.W., Christl, M., Kasper, H.U., Wieler, R., Baroni, C., 2009. Multiple cosmogenic nuclides document complex Pleistocene exposure history of glacial drifts in Terra Nova Bay (northern Victoria Land, Antarctica). Quaternary Research 71 (1), 83–92.

Draxler, R.R., Rolph, G.D., 2012. HYSPLIT (HYbrid Single-particle Lagrangian Integrated Trajectory). NOAA Air Resources Laboratory, Silver Spring, MD. Model access via NOAA ARL READY Website. http://ready.arl.noaa.gov/HYSPLIT.php.

Elliot, D.H., Fleming, T.H., Haban, M.A., Siders, M.A., 1995. Petrology and mineralogy of the Kirkpatrick basalt and Ferrar Dolerite, Mesa Range region, north Victoria Land, Antarctica. In: Elliot, D.H., Blaisdell, G.L. (Eds.), Contributions to Antarctic Research IV. Antarct. Res. Ser., vol. 67. AGU, Washington, D.C., pp. 103–141. http://dx.doi.org/10.1029/AR067p0103.

Faure, G., 1986. Principles of Isotope Geology, second ed. Wiley, New York.

Faure, G., Mensing, T.M., 2010. The Transantarctic Mountains. Rocks, Ice, Meteorites and Water. Springer, Dordrecht.

Feng, J.-L., Zhu, L.-P., Zhen, X.-L., Hu, Z.-G., 2009. Grain size effect on Sr and Nd isotopic compositions in eolian dust: implications for tracing dust provenance and Nd model age. Geochemical Journal 43, 123–131.

Fleming, T.H., Foland, K.A., Elliot, D.H., 1995. Isotopic and chemical constraints on the crustal evolution and source signature of the Ferrar magmas, north Victoria Land, Antarctica. Contributions to Mineralogy and Petrology 121, 217–236.

Frezzotti, M., Pourchet, M., Flora, O., Gandolfi, S., Gay, M., Urbini, S., Vincent, C., Becagli, S., Gragnani, R., Proposito, M., Severi, M., Traversi, R., Udisti, R., Fily, M.,

2004. New estimations of precipitation and surface sublimation in East Antarctica from snow accumulation measurements. Climate Dynamics 23, 803–813. http://dx.doi.org/10.1007/s00382-004-0462-5.
Frezzotti, M., Pourchet, M., Flora, O., Gandolfi, S., Gay, M., Urbini, S., Vincent, C., Becagli, S., Gragnani, R., Proposito, M., Severi, M., Traversi, R., Udisti, R., Fily, M., 2005. Spatial and temporal variability of snow accumulation in East Antarctica from traverse data. Annals of Glaciology 51 (172), 113–124.
Frezzotti, M., Urbini, S., Proposito, M., Scarchilli, C., Gandolfi, S., 2007. Spatial and temporal variability of surface mass balance near Talos Dome, East Antarctica. Journal of Geophysical Research 112, FO2032.
Gabrielli, P., Wegner, A., Petit, J.R., Delmonte, B., De Deckker, P., Gaspari, V., Fischer, H., Ruth, U., Kriews, M., Boutron, C., Cescon, P., Barbante, C., 2010. A major glacial–interglacial change in aeolian dust composition as inferred from Rare Earth Elements in Antarctic ice. Quaternary Science Reviews 29 (1–2), 265–273. http://dx.doi.org/10.1016/j.quascirev.2009.09.002.
Grousset, F.E., Biscaye, P.E., Revel, M., Petit, J.R., Pye, K., Jossaume, S., Jouzel, J., 1992. Antarctic (Dome C) ice-core dust at 18 k.y. B.P.: isotopic constraints and origins. Earth and Planetary Science Letters 111, 175–182.
Hall, B.L., 2009. Holocene glacial history of Antarctica and the sub-Antarctic islands. Quaternary Science Reviews 28 (21–22), 2213–2230.
Hall, B.L., Hoelzel, A.R., Baroni, C., Denton, G.H., Le Boeuf, B.J., Overturf, B., Töpf, A.L., 2006. Holocene elephant seal distribution implies warmer-than-present climate in the Ross Sea. Proceedings of the National Academy of Sciences of the United States of America 103 (27), 10213–10217.
Hong, S., Kim, Y., Boutron, C.F., Ferrari, C.P., Petit, J.R., Barbante, C., Rosman, K.J.R., Lipenkov, V.Y., 2003. Climate-related variations in lead concentrations and sources in Vostok Antarctic ice from 65,000 to 240,000 years BP. Geophysical Research Letters 30 (22), 2138.
Kellogg, D.E., Kellogg, T.B., 1996. Diatoms in South Pole ice: Implications for eolian contamination of Sirius Group deposits. Geology 24 (2), 115–118.
Kohfeld, K.E., Harrison, S.P., 2001. DIRTMAP: the geological record of dust. Earth-Science Reviews 54 (1–3), 81–114.
Krinner, G., Petit, J.R., Delmonte, B., 2010. Altitude of atmospheric tracer transport towards Antarctica in present and glacial climate. Quaternary Science Reviews 29 (1–2), 274–284. http://dx.doi.org/10.1016/j.quascirev.2009.06.020.
Lanci, L., Delmonte, B. Magnetic properties of aerosol dust in peripheral and inner Antarctic ice cores as a proxy for dust Provenance. Global and Planetary Change, Special Issue “Magnetic Minerals in Sediments”, in press.
Li, F., Ginoux, P., Ramaswamy, V., 2008. Distribution, transport, and deposition of mineral dust in the Southern Ocean and Antarctica: contribution of major sources. Journal of Geophysical Research 113, D10207. http://dx.doi.org/10.1029/2007JD009190.
Lambert, F., Delmonte, B., Petit, J.R., Bigler, M., Kaufmann, P.R., Hutterli, M., Stocker, T.F., Ruth, U., Steffensen, J.P., Maggi, V., 2008. New constraints on the dust-climate couplings from the 800,000-year EPICA Dome C ice core. Nature 452 (7187), 616–619. http://dx.doi.org/10.1038/nature06763.
Lancaster, N., 2002. Flux of eolian sediment in the McMurdo dry Valleys, Antarctica: a preliminary assessment. Arctic, Antarctic, and Alpine Research 34 (3), 318–323.
Magand, O., Frezzotti, M., Pourchet, M., Stenni, B., Genoni, L., Fily, M., 2004. Climate variability along latitudinal and longitudinal transects in East Antarctica. Annals of Glaciology 39, 351–358. http://dx.doi.org/10.3189/172756404781813961.
Maher, B.A., Prospero, J.M., Mackie, D., Gaiero, D., Hesse, P.P., Balkanski, Y., 2010. Global connections between aeolian dust, climate and ocean biogeochemistry at the present day and at the last glacial maximum. Earth Science Reviews 99 (1–2), 61–97. http://dx.doi.org/10.1016/j.earscirev.2009.12.001.
Marino, F., Castellano, E., Ceccato, D., De Deckker, P., Delmonte, B., Ghermandi, G., Maggi, V., Petit, J.R., Revel-Rolland, M., Udisti, R., 2008. Defining the geochemical composition of the EPICA Dome C ice core dust during the last glacial/interglacial cycle. Geochemistry Geophysics Geosystems 9, Q10018. http://dx.doi.org/10.1029/2008GC002023.
Marino, F., Castellano, E., Nava, S., Chiari, M., Ruth, U., Wegner, A., Lucarelli, F., Udisti, R., Delmonte, B., Maggi, V., 2009. Coherent composition of glacial dust on opposite sides of the East Antarctic Plateau inferred from the deep EPICA ice cores. Geophysical Research Letters 36 (23). http://dx.doi.org/10.1029/2009GL040732. art. no. L23703.
Matsumoto, A., Hinkley, T.K., 2001. Trace metal suites in Antarctic pre-industrial ice are consistent with emissions from quiescent degassing of volcanoes worldwide. Earth and Planetary Science Letters 186, 33–43.
McKay, R.M., Barrett, P.J., Harper, M.A., Hannah, M.J., 2008. Atmospheric transport and concentration of diatoms in surficial and glacial sediments of the Allan Hills, Transantarctic Mountains. Palaeogeography, Palaeoclimatology, Palaeoecology 260 (1–2), 168–183.
McKenna Neuman, C., 2004. Effects of temperature and humidity upon the transport of sedimentary particles by wind. Sedimentology 51 (1), 1–17. http://dx.doi.org/10.1046/j.1365-3091.2003.00604.x.
Meneghel, M., Bondesan, A., Salvatore, M.C., Orombelli, G., 1999. A model of the glacial retreat of upper Rennick Glacier, Victoria Land, Antarctica. Annals of Glaciology 29, 225–230.
Narcisi, B., Petit, J.R., Delmonte, B., Basile-Doelsch, I., Maggi, V., 2005. Characteristics and sources of tephra layers in the EPICA-dome C ice record (East Antarctica): Implications for past atmospheric circulation and ice core stratigraphic correlations. Earth and Planetary Science Letters 239 (3–4), 253–265.
Narcisi, B., Petit, J.R., Delmonte, B., Scarchilli, C., Stenni, B., 2012. A 16,000-yr tephra framework for the Antarctic ice sheet: a contribution from the new Talos Dome core. Quaternary Science Reviews 49, 52–63.
Oberholzer, P., Baroni, C., Schaefer, J.M., Orombelli, G., Ochs, S.I., Kubik, P.W., Baur, H., Wieler, R., 2003. Limited Pliocene/Pleistocene glaciation in Deep Freeze Range, northern Victoria Land, Antarctica, derived from in situ cosmogenic nuclides. Antarctic Science 15 (4), 493–502.
Oberholzer, P., Baroni, C., Salvatore, M.C., Baur, H., Wieler, R., 2008. Dating late Cenozoic erosional surfaces in Victoria Land, Antarctica, with cosmogenic neon in pyroxenes. Antarctic Science 20 (1), 89–98.
Orombelli, G., Baroni, C., Denton, G.H., 1990. Late Cenozoic glacial history of the Terra Nova Bay region, northern Victoria Land, Antarctica. Geografia Fisica e Dinamica Quaternaria 13 (2), 139–163.
Petit, J.R., Jouzel, J., Raynaud, D., Barkov, N.I., Barnola, J.M., Basile, I., Bender, M., Chappellaz, J., Davis, M., Delaygue, G., Delmotte, M., Kotlyakov, V.M., Legrand, M., Lipenkov, V.Y., Lorius, C., Pepin, L., Ritz, C., Saltzman, E., Stievenard, M., 1999. Climate and atmospheric history of the past 420000 years from the Vostok ice core, Antarctica. Nature 399, 429–436.
Petit, J.R., Delmonte, B., 2009. A model for large glacial–interglacial climate-induced changes in dust and sea salt concentrations in deep ice cores (central Antarctica): palaeoclimatic implications and prospects for refining ice core chronologies. Tellus 61B, 768–790.
Proposito, M., Becagli, S., Castellano, E., Flora, O., Genoni, L., Gragnani, R., Stenni, B., Traversi, R., Udisti, R., Frezzotti, M., 2002. Chemical and isotopic snow variability along the 1998 ITASE traverse from Terra Nova Bay to Dome C, East Antarctica. Annals of Glaciology 35 (1), 187–194.
Revel-Rolland, M., De Deckker, P., Delmonte, B., Hesse, P.P., Magee, J.W., Basile-Doelsch, I., Grousset, F., Bosch, D., 2006. Eastern Australia: a possible source of dust in East Antarctica interglacial ice. Earth and Planetary Science Letters 249, 1–13. http://dx.doi.org/10.1016/j.epsl.2006.06.028.
Scarchilli, C., Frezzotti, M., Ruti, P.M., 2011. Snow precipitation at four ice core sites in East Antarctica: provenance, seasonality and blocking factors. Climate Dynamics 37, 2107–2125. http://dx.doi.org/10.1007/s00382-010-0946-4.
Schafer, J.M., Ivy-Ochs, S., Wieler, R., Leya, I., Baur, H., Denton, G.H., Schluchter, C., 1999. Cosmogenic noble studies in the oldest landscape on earth: surface exposure ages of the Dry Valleys, Antarctica. Earth and Planetary Science Letters 167 (3–4), 215–226.
Schlosser, E., Oerter, H., Masson-Delmotte, V., Reijmer, C., 2008. Atmospheric influence on the deuterium excess signal in polar firn: Implications for ice-core interpretation. Journal of Glaciology 54 (184), 117–124. http://dx.doi.org/10.3189/002214308784408991.
Severi, M., Udisti, R., Becagli, S., Stenni, B., Traversi, R., 2012. Volcanic synchronisation of the EPICA-DC and TALDICE ice cores for the last 42 kyr BP. Climate of the Past 8, 509–517. http://dx.doi.org/10.5194/cp-8-509-2012.
Sinclair, K.E., Bertler, N.A.N., Trompetter, W.J., 2010. Synoptic controls on precipitation pathways and snow delivery to high-accumulation ice core sites in the Ross Sea region, Antarctica. Journal of Geophysical Research 115, D22112. http://dx.doi.org/10.1029/2010JD014383.
Stenni, B., Buiron, D., Frezzotti, M., Albani, S., Barbante, C., Bard, E., Barnola, J.M., Baroni, M., Baumgartner, M., Bonazza, M., Capron, E., Castellano, E., Chappellaz, J., Delmonte, B., Falourd, S., Genoni, L., Iacumin, P., Jouzel, J., Kipfstuhl, S., Landais, A., Lemieux-Dudon, B., Maggi, V., Masson-Delmotte, V., Mazzola, C., Minster, B., Montagnat, M., Mulvaney, R., Narcisi, B., Oerter, H., Parrenin, F., Petit, J.R., Ritz, C., Scarchilli, C., Schilt, A., Schüpbach, S., Schwander, J., Selmo, E., Severi, M., Stocker, T.F., Udisti, R., 2011. Expression of the bipolar seesaw in Antarctic climate records during the last deglaciation. Nature Geoscience 4, 46–49. http://dx.doi.org/10.1038/NGEO1026.
Strasky, S., Di Nicola, L., Baroni, C., Salvatore, M.C., Baur, H., Kubik, P.W., Schlüchter, C., Wieler, R., 2009. Surface exposure ages imply multiple low-amplitude Pleistocene variations in East Antarctic Ice Sheet, Ricker Hills, Victoria Land. Antarctic Science 21 (1), 59–69.
Summerfield, M.A., Sugden, D.E., Denton, G.H., Marchant, D.R., Cockburn, H.A.P., Stuart, F.M., 1999. Cosmogenic isotope data support previous evidence of extremely low rates of denudation in the Dry Valleys region, southern Victoria Land, Antarctica. Geol. Soc. Lond. Spec. Publ. 162, 255–267.
Tedrow, J.C.F., Ugolini, F., 1966. In: Antarctic Soils, Tedrow, J.C.F. (Eds.), Antarctic Soils and Soil Forming Processes. American Geophysical Union, pp. 161–176.
Traversi, R., Becagli, S., Castellano, E., Largiuni, O., Migliori, A., Severi, M., Frezzotti, M., Udisti, R., 2004. Spatial and temporal distribution of environmental markers from coastal to plateau areas in Antarctica by firn core chemical analysis. International Journal of Environmental Analytical Chemistry 84, 457–470.
Vallelonga, P., Gabrielli, P., Rosman, K.J.R., Barbante, C., Boutron, C.F., 2005. A 220 kyr record of Pb isotopes at Dome C Antarctica from analyses of the EPICA ice core. Geophys. Res. Lett 32 (1), L01706.
Vallelonga, P., Gabrielli, P., Balliana, E., Wegner, A., Delmonte, B., Turetta, C., Burton, G., Vanhaecke, F., Rosman, K.J.R., Hong, S., Boutron, C.F., Cescon, P., Barbante, C., 2010. Lead isotopic compositions in the EPICA Dome C ice core and Southern Hemisphere Potential Source Areas. Quaternary Science Reviews 29 (1–2), 47–55. http://dx.doi.org/10.1016/j.quascirev.2009.06.019.
Van de Velde, K., Vallelonga, P., Candelone, J.-P., Rosman, K.J.R., Gaspari, V., Cozzi, G., Barbante, C., Udisti, R., Cescon, P., Boutron, C.F., 2005. Pb isotope record over one century in snow from Victoria Land, Antarctica. Earth Planet. Sci. Lett. 232, 95–108.
Wegner, A., Gabrielli, P., Wilhelms-Dick, D., Ruth, U., Kriews, M., De Deckker, P., Barbante, C., Cozzi, G., Delmonte, B., Fischer, H., 2012. Change in dust variability in the Atlantic sector of Antarctica at the end of the last deglaciation. Climate of the Past 8 (1), 135–147. http://dx.doi.org/10.5194/cp-8-135-2012.
Yung, Y.L., Lee, T., Wang, C.H., Shieh, Y.T., 1996. Dust: a diagnostic of the hydrologic cycle during the Last Glacial Maximum. Science 271, 962–963.